

Canadian Society for Pharmaceutical Sciences Abstracts of posters presented at the 2023rd Symposium and General Meeting

May 24-26, Toronto Convention Centre



The 2023 CSPA annual conference was held in the Toronto Convention Centre on May 24-26. The Symposium showcased small and large Pharma, regulatory partners, and academia building and broadening pharmaceutical sciences in Canada from discovery to recovery.

Invited speakers presented in the following sessions:

- Presentations from the Canadian Pharmaceutical Industry
- Career Connections in Delivery Science & Technology
- Young Scientist Network - Issues to Consider Before Launching a Start-up
- Gene Therapy
- Drug Delivery and Nanomedicines
- Engineered Cell Therapy
- Bench to Business
- Molecular Imaging and Personalized Medicine
- AI and Computer Technology in the Sciences



Lipopolymer Mediated RNAi Therapy Targeting FLT3 in Acute Myeloid Leukemia

Aysha Ansari¹, Remant Kc¹, Mohammad Nasrullah¹, Daniel Sundaram¹, Luis Burbano¹, Joseph Brandwein¹, Xiaoyan Jiang¹, Hasan Uludag¹

¹University of Alberta, Edmonton, AB

Purpose: Approximately 25% of newly diagnosed AML patients display an internal tandem duplication (ITD) in the *fms-like tyrosine kinase 3* (*FLT3*) gene. Although both multi-targeted and FLT3 specific tyrosine kinase inhibitors (TKIs) are being utilized for clinical therapy, drug resistance, short remission periods, and high relapse rates are challenges that still need to be tackled [1]. RNA interference (RNAi), mediated by short interfering RNA (siRNA) presents an alternative therapeutic platform with the potential of personalization. The success of RNAi therapy to a great extent is dictated by the siRNA delivery vehicle employed. This study explored the use of a lipid-substituted low molecular weight polyethyleneimine (lipopolymer) for delivering FLT3 siRNA in FLT3-ITD positive AML models and assess the efficacy of combining this treatment with clinical drugs.

Methods: Cell proliferation rates were determined by trypan blue exclusion cell counting. Apoptosis was measured by Annexin V/FITC and propidium iodide staining. qPCR was conducted to quantify *FLT3* mRNA transcript levels. FLT3 protein levels were measured by flow cytometry by staining with an anti-FLT3 antibody. MV4-11 subcutaneous xenografts were generated in NCG (ABL/VAF) mice. Lipopolymer/siRNA complexes were administered at a dose of 1 mg/kg intravenously (via tail-vein), while gilteritinib was injected intraperitoneally at a dose of 5 mg/kg.

Results: Low molecular weight polyethyleneimine (PEI) polymers were modified with aliphatic lipids to yield lipopolymers that self-assembled into nanocomplexes with siRNA. Treatment of MV4-11 cells with lipopolymer/FLT3 siRNA nanocomplexes resulted in prominent reduction in cell proliferation rates and induction of apoptosis. Quantitative analysis of relative mRNA transcript levels revealed downregulation of FLT3 gene, which was accompanied by a similar decline in FLT3 protein levels. The effect of combining lipopolymer/FLT3 siRNA treatment with

daunorubicin and FLT3 targeting TKI gilteritinib led to a significant augmentation of anti-leukemic activity. Subsequently, gilteritinib was explored in combination with lipopolymer/FLT3 siRNA nanocomplexes *in vivo*. A significant reduction in tumor volume was observed in the combination treated tumors compared to gilteritinib alone treated tumors. The combination therapy significantly increased median survival to 65 days as compared to 45 days with gilteritinib treatment alone.

Conclusion: The findings of this study demonstrate the promising potential of RNAi implemented with lipopolymer nanocomplexes for AML molecular therapy.

References

J Hematol Oncol 2020 13: 155

A Disease Progression Based Nonlinear Mixed-Effects Pharmacodynamic Model for Improving Long-Term Renal Transplant Outcomes through Personalized Immunosuppressant Dosing

Yao Chen¹, Harvey Wong¹

¹University of British Columbia

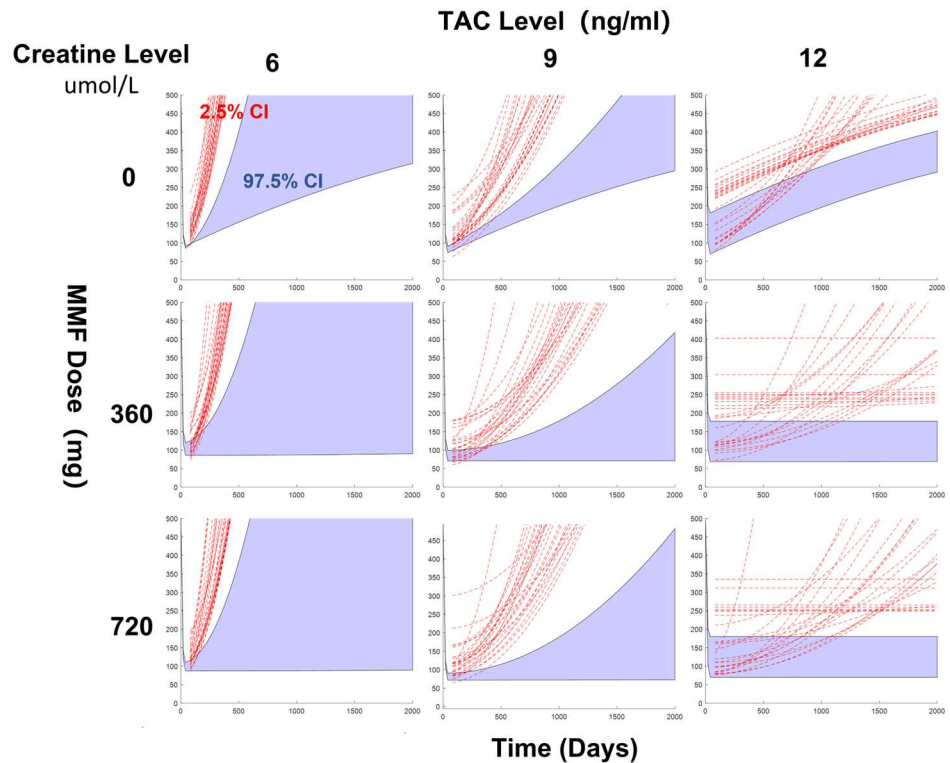
Background: Co-administering a calcineurin inhibitor (CNI) like Tacrolimus (Tac) and purine synthase inhibitor (PSI) like Mycophenolate (MMF) is essential for preventing acute transplant rejection (<1 Year), but novel immunosuppressants and monitoring have failed to improve chronic rejection (>1 year). Studying and investigating the long-term effects of immunosuppressants is challenging due to the limited, dichotomous nature of current research and the lack of a viable longitudinal biomarker. The emerging field of model-informed approaches offers opportunities to bridge this gap.

Methodology: Our investigation of the McGill transplant retrospective biorepository cohort in Quebec (n=450) uses a centralized high-performance computing (HPC) platform for parallel computing, secure data storage, and application hosting. A nonlinear mixed-effect model (NONMEM 7.4.3) with disease progression structure characterizes the immunosuppressant effect on creatine level (physiological biomarker for

renal function). Monte Carlo simulation (n=2000, MATLAB) emulates fixed dosing and dose reduction scenarios and produce visual/statistical reference of renal function change.

Result: Preliminary analysis identified the correlation between immunosuppressant dose/exposure and long-term transplant outcome (log rank, $p=0.0056$). Concentration/Dose-dependent effect ($\Theta_{\text{Tac_conc}}$, $\Theta_{\text{MMF_Dose}}$) and their interindividual variability (Ω_{Tac} , Ω_{MMF}) on renal function was characterized in combined dosing scenario with time-dependent factor for tolerance captured ($\Theta_{\text{Time_Tac}}$, $\Theta_{\text{Time_MMF}}$).

Conclusion: This study offers a model-informed framework for evaluating immunosuppressants effect on long-term renal function change, with the aim of assisting future clinical studies and practices. It indicates a dose/concentration-dependent effect of immunosuppressants on renal function that varies by individual. Our future investigation will identify patient characteristics that contribute to this variability, thereby enabling individualized immunosuppressant dosing.



Computer Simulation as a Tool to Investigate Pharmaceutical Protein/Peptide Delivery by Polymers

Sako Mirzaie¹, Amin GhavamiNejad¹, Brian Lu¹, Jackie Fule Liu¹, Adria Giacca², Xiao Yu (Shirley) Wu¹

¹Advanced Pharmaceutics and Drug Delivery Laboratory, Leslie Dan Faculty of Pharmacy, University of Toronto., ²Department of Physiology, Faculty of Medicine, University of Toronto.

Purpose: Insulin therapy is essential for individuals with Type 1 diabetes and about 30 % of those with advanced type 2 diabetes, but hypoglycemia is a potentially fatal side effect. The Wu lab has created a microneedle patch to prevent hypoglycemia, delivering glucagon and PRL 2903 through biocompatible polymers. However, glucagon chains can form fibrils that increase cytotoxicity and decrease bioavailability, while PRL 2903 loses bioactivity when exposed to UV irradiation. The study aims to use molecular dynamics (MD) modeling to investigate how synthesized polymers stabilize glucagon and PRL 2903. This research has the potential to improve the efficacy and safety of the microneedle patch for hypoglycemia prevention.

Method: The methacrylated HA (MeHA) and sulfobetaine aminophenylbronic acid carboxybetaine (SB-ABA-CB) polymers were constructed by AmberTools 17. PRL 2903 was constructed in HyperChem Professional 8.0 software. The glucagon structure was retrieved from the protein data bank. MD simulations were conducted by Desmond software. The results were analyzed by in-house Python scripts. All the simulations were conducted by Wu's lab GPU-equipped workstations.

Results: The study found that the presence of MeHA and SB-ABA-CB polymers reduced local and global fluctuations in PRL 2903 and glucagon, respectively. MeHA also increased the intra-hydrogen bonding of PRL 2903, providing greater stability and restricting its torsion angles. On the other hand, SB-ABA-CB polymer prevented glucagon

aggregation and fibrillation by shielding the peptide surface and formation of multiple hydrogen bonds with polar and charged amino acid residues on the glucagon molecule.

Conclusion: These findings suggest that the synthesized polymers may be effective in stabilizing glucagon and PRL 2903, enhancing their bioavailability and reducing the risk of hypoglycemia. Our MD results showed good consistency with our relevant experimental data.

The alteration of p16 expression by reduction of global DNA methylation using DNMT inhibitors on gastric cancer cell lines
Wenxia Luo¹, Olufola Ige¹, Thordur Hendrickson-Rebizant¹, Ted Lakowski¹

¹University of Manitoba, Winnipeg, MB

Purpose: Cytosine methylation of promoter CpG islands suppresses gene expression and is catalyzed by DNA methyltransferases (DNMT). This methylation is known as an epigenetic modification to DNA, and promoter hypermethylation suppresses expression of the tumor suppressor cyclin-dependent kinase inhibitor 2A (p16) is involved in some types of gastric cancer, which is one of the most common types of cancer.

Methods: We developed and validated a LC-MS/MS method to quantify DNA methylation and other modified DNA bases using synthetic 20mer dsDNA oligonucleotides, each containing a single modified nucleotide. We treated different gastric cells lines by two DNMT inhibitors: decitabine approved by FDA and a novel inhibitor GSK3685032 and evaluated their viability, DNA methylation, p16 expression.

Results: Decitabine decreased the total methylation status for all cell lines studied. GSK3685032 decreased the total methylation status in all cell lines initially, then the total methylation increased with increasing GSK3685032 concentrations. The alteration of DNA methylation status is consistent with p16 expression alterations shown for SNU 719 and AGS with treatment of decitabine and GSK3685032. However, in MKN

45, there was no expression of p16.

Conclusion: Promoter hypermethylation is one of the factors affecting p16 expression in some gastric cancer cell lines. SNU 719 and AGS are DNMT inhibitor-sensitive cell lines for p16 and are appropriate models for the link between p16 expression and CpG methylation in humans. The parabolic DNA methylation change for GSK3685032 suggests its inhibition effects on DNMT may influence expressions of enzymes that add or remove methylation marks on DNA.

References

1. Hum Genet 1989 83(2) 155-158.
2. Med Oncol. 2015 32(4) 92

Method Development and Validation of Reverse-Phase HPLC Assay for Quantification of Mycophenolic Acid and Plasma Extraction Procedures

Adrienne Nagy¹, Deborah Michel¹, Ellen Wasan¹

¹University of Saskatchewan

We have developed modified release formulations of the immunosuppressant drug mycophenolate mofetil (MMF) to simplify dosing regimens for enhancing treatment adherence in organ transplant patients. In preparation for preclinical pharmacokinetic studies, the objective of this project was to develop a validated reverse-phase high-pressure liquid chromatography (HPLC) assay for the quantification of mycophenolic acid (MPA) extracted from rat plasma. Mycophenolic acid is the active metabolite of mycophenolate mofetil. Initial assay conditions were based on a reverse-phase HPLC assay developed for quantification of parent compound mycophenolate mofetil (MMF) in mobile phase. Hypotheses based on the chemical differences between MPA and MMF were formulated to guide method development: decreasing mobile phase pH will improve analyte peak uniformity, gradient flow conditions will improve column retention and timely elution, and acetonitrile as organic mobile phase will improve elution strength. An optimized extraction procedure was developed from rat plasma using Captiva Agilent EMR-Lipid 96-Well Plates, with >90% extraction recovery

accounting for matrix effect. The validated HPLC assay for quantification of MPA extracted from rat plasma employed a gradient flow mobile phase comprised of TFA 0.03% in water, and acetonitrile on a Phenomenex Luna 5 μ m C8 100 Å 30 x 2mm column at 37°C. Median retention time was 2.57 +/- 0.01 min with <1% difference inter and intra-day, and the linear range was 1-45 μ g/mL with a detection limit of 0.4 μ g/mL, and linearity (r^2) >0.99. This high sensitivity encompasses the expected range of plasma concentrations anticipated for the planned pharmacokinetic analysis. Inter-day accuracy varied from 92-118% for the lowest limit of quantitation (LLOQ), and 85-114% for quality controls; inter-day precision was <15%.

Acknowledgements: AN is the recipient of a CSPS National Undergraduate Student Research Award, and a summer student fellowship from the NanoMedicines Innovation Network, a National Centre of Excellence (NCE)

Impact of Vitamin C Supplementation on Oxidizing Cytotoxic Anti-Cancer Therapy (ACT): A Systematic Review

Bhawani Jain¹, Emilia Main², Victoria Bugaj², Maria Marchese², Yoonna Lee², Gloria (Ji Hee) Choi², Carlo DeAngelis^{1, 2, 3}, Christine Peragine²

¹University of Waterloo School of Pharmacy, ²Odette Cancer Centre, Sunnybrook Health Sciences Centre, ³University of Toronto, Leslie Dan Faculty of Pharmacy

Background

Pharmacists often advise patients taking Vitamin C (VC) to avoid concurrent use with oxidizing anticancer therapy (ACT) due to VC's antioxidant properties. Our systemic review exploring the impact of melatonin supplementation on the efficacy of oxidizing anticancer therapy (ACT) found no negative effect on overall response (OR) or overall survival (OS); however, a similar review of focused on VC has not been conducted.

Purpose

This systematic review summarizes available data from randomized

controlled trials (RCTs) to determine if VC supplementation negatively impacts efficacy of oxidizing cytotoxic ACT.

Hypothesis

Taking Vitamin C supplementation concurrently with oxidizing cytotoxic ACT does not negatively impact ACT efficacy as measured by progression-free survival (PFS), OR, and OS.

Methods

A search strategy to identify target English full-text articles was created in collaboration with the hospital librarian in OVID MEDLINE, EMBASE, and PubMed databases. Studies of RCTs were included based on the following criteria: (1) cancer patient population, (2) experimental arm received oxidizing ACT + VC, (3) control arm received oxidizing ACT \pm placebo, and (4) progression free survival (PFS), OR, and OS reported as outcomes. Covidence software was used to screen and extract data. RevMan 5 software was used to calculate risk differences (RD) for outcomes when data was available in ≥ 3 studies. Noninferiority (NI) of VC supplementation was assessed using an NI margin of ± 0.10 . Cochrane risk-of-bias tool for RCTs (RoB 2) was applied to included studies.

Results

Of the 666 articles analyzed, 5 relevant RCTs were identified. Three studies reported OR data (RD_{OR} 0.02, 95% CI -0.06 to 0.10), 4 studies reported 1-year and 2-year OS ($RD_{mortality,1y}$ -0.07, 95% CI -0.13 to 0.00; $RD_{mortality,2y}$ -0.02, 95% CI -0.09 to 0.05). The target upper or lower bound of the CIs did not cross the NI margin for each outcome analyzed. As only 2 studies reported PFS, this outcome was not able to be assessed. Potential moderate risk of bias was identified.

Impact

Findings suggest combination therapy of VC + ACT is non-inferior to ACT monotherapy for OR and OS outcomes. Despite the small number of RCTs identified and potential risk of bias, our exclusion of nonrandomized studies and consistency with our ACT \pm melatonin systematic review results provide confidence that VC supplementation

does not compromise ACT efficacy.

Exposure-Toxicity Relationships of Tacrolimus on the Development of Post-Transplant Diabetes in Renal Transplant Patients

Angel Nong¹, Johnny Zhu¹, Tony Kiang¹

¹Faculty of Pharmacy and Pharmaceutical Sciences, University of Alberta, Edmonton

Purpose: Tacrolimus is the mainstay of the three-drug immunosuppressive regimen taken by kidney transplant patients. More so than other anti-rejection medications, tacrolimus has been associated with the development of post-transplant diabetes mellitus (PTDM) where patients are diagnosed Type 2 diabetes within the first few months post-transplantation. PTDM is a concerning complication as it is associated with greater risks of cardiovascular-related deaths, infections, and renal graft dysfunction. However, it is unclear whether a concentration-toxicity relationship exists and if higher blood tacrolimus levels can lead to an increased risk.

Methods: A scoping literature review of primary studies that examined the concentration-toxicity relationship between tacrolimus and PTDM in patients receiving kidney transplants was conducted. PubMed, EMBASE and Medline were searched (limit being English language), where 51 primary studies were included. Data was extracted and ranked using criteria defined *a priori* (e.g., definition of PTDM, transplant regimen, patient population, pharmacokinetic data, potential confounding clinical variables). Data were extracted and analyzed independently by two researchers (AN and JZ).

Results: Mix findings which supported (N=26) and refuted (N=25) the relationship between tacrolimus plasma trough levels and PTDM were observed. A few studies suggested that trough concentrations >8 ng/mL may increase the risk of PTDM. Aside from tacrolimus trough blood levels, clinical variables such as age (>45 years), family history of diabetes, impaired fasting glucose pre-transplant, corticosteroids, increased body mass index, and race were also associated with PTDM

development.

Conclusion: A potential association between tacrolimus trough concentration and the development of PTDM is evident in our primary literature critique. Further analyses are currently being conducted to evaluate the strength of the identified associations and factors influencing the relationship between tacrolimus and PTDM.

Angel Nong is the recipient of the 2023 CSPS National Undergraduate Student Research Award representing the University of Alberta.

Intracellular trafficking of the scavenger receptor CD36 via the endosomal-lysosomal pathway in macrophages

Catherine Lê¹, Mukandila Mulumba¹, Emmanuelle Schelsohn², William Lubell³, Sylvie Marleau¹, Huy Ong¹

¹Faculty of Pharmacy, University of Montreal, ²Faculty of Pharmacy, University of Geneva, ³Department of Chemistry, University of Montreal

Purpose: It is known that CD36/SR-B2 scavenger receptor interaction with oxLDL results in its internalization, and in the initiation of intracellular proinflammatory and proatherogenic signaling cascades in macrophages. The aim of our study is to investigate the intracellular disposition of the CD36 receptor after its binding to the cyclic azapeptide MPE-298, an anti-atherosclerotic synthetic ligand featuring high affinity binding towards CD36. We hypothesize that MPE-298 promotes the internalization of CD36 in macrophages and its intracellular trafficking involving the endosomal-lysosomal pathway.

Methods: J774 macrophages, transfected with a murine CD36-GFP plasmid, were incubated with 100 nM MPE-298 in a time-course study ranging from 5 to 15 minutes. Different endocytosis compartments were labelled with specific antibodies of endocytic markers to study their colocalization with CD36, including early (EEA-1), late (Rab7) and recycling (Rab11) endosomes, as well as lysosomes (LAMP-1). Colocalization of CD36 with endocytic markers was assessed using the ImageJ Jacop plugin.

Results: Following exposure to MPE-298, we observed that the CD36 receptor colocalizes rapidly within early endosomes, reaching a peak after 10 minutes of incubation with MPE-298, followed by a slight colocalization decrease at 15 minutes. CD36 was also found to colocalize with late endosomes and lysosomes, the colocalization reaching a plateau after 15 minutes with MPE-298. On the other hand, CD36 displays a low colocalization with recycling endosomes.

Conclusion: This study shows that binding of the MPE-298 azapeptide to the membrane CD36 receptor induces rapid endocytosis of the scavenger receptor in the macrophages. The internalized fluorescent tracer-labelled CD36 was found to accumulate rapidly in early endosomes, late endosomes and lysosomes, but not in recycling endosomes. These results show the role of the intracellular trafficking of CD36 to lysosomes without recycling CD36 back to the membrane, contributing to the reduction of oxLDL uptake, leading to the reduction of inflammation and atherogenic progression.

Role of Cytochrome P450 in Aldehyde Oxidase Inactivation by Epidermal Growth Factor Receptor-Tyrosine Kinase Inhibitors

Sarah Smit¹, Brandon MacDonald¹, Aik Jiang Lau²

¹Student, ²Principle Investigator

Purpose: An increasing number of drugs and drug candidates are metabolized by a cytosolic drug-metabolizing enzyme, aldehyde oxidase (AOX1). However relatively little is known about the mechanism of AOX1 inactivation and the functional interaction between AOX1 and drugs in clinical use. In this study, we investigated whether gefitinib and its metabolites, an epidermal growth factor receptor tyrosine kinase inhibitor, inactivate AOX1 by a mechanism involving the cytochrome P450 (CYP) enzymes.

Methods: We developed and validated an ultra-high performance liquid chromatography-tandem mass spectrometric (UPLC-MS/MS) method to quantify AOX1-catalyzed carbazeran 4-oxidation and *O*⁶-benzylguanine 8-oxidation. Time-dependent inactivation assays were conducted by pre-incubating the drugs/metabolites with human liver S9 fraction (150

donors) at 37°C for an optimized duration, and the remaining AOX1 activity (carbazeran 4-oxidation or *O*⁶-benzylguanine 8-oxidation) was assessed by UPLC-MS/MS.

Results: Gefitinib and *O*-desmethylgefitinib, but not *O*-desmorpholinopropylgefitinib, decreased carbazeran 4-oxidation, but not *O*⁶-benzylguanine 8-oxidation, in a time- and substrate-dependent manner in human liver S9 fraction, indicating the involvement of the morpholine ring of gefitinib in the inactivation. The decrease in AOX1-catalyzed carbazeran 4-oxidation occurred only in the presence of NADPH but not in the absence of NADPH, indicating that NADPH-dependent CYP enzymes are necessary for the inactivation. This time-dependent inactivation was abolished by *O*-desmorpholinopropylgefitinib (a competitive AOX1 inhibitor), but not *O*⁶-benzylguanine (an AOX1 substrate that showed AOX1 inactivation), suggesting that the inactivation occurred at the AOX1 active site.

Conclusion: Gefitinib and *O*-desmethylgefitinib, but not *O*-desmorpholinopropylgefitinib, inactivate AOX1 indirectly in the presence of NADPH-dependent CYP enzymes. The findings suggest an interplay between the dual functionality of cytochrome P450 and AOX1 in regulating drug metabolism, and the potential effect of gefitinib on other drugs and chemicals metabolized by AOX1.

Acknowledgements: Funding was provided by the Dalhousie Pharmacy Endowment Fund. MacDonald and Smit are recipients of the CSPS student undergraduate award.

Predictive performance of pharmacokinetic models of rifampicin in tuberculosis patients

Henri Fournier¹, Romain Guilhaumou², Chantale Simard^{1,3}, Amélie Marsot^{4,5,6}

¹Faculté de Pharmacie, Université Laval, Québec, QC, Canada, ²Service de Pharmacologie Clinique et Pharmacovigilance, Hôpital de la Timone, Assistance Publique des Hôpitaux de Marseille, Marseille, France, ³Centre de Recherche, Institut universitaire de cardiologie et de pneumologie de

Québec, Québec, QC, Canada, ⁴Faculté de Pharmacie, Université de Montréal, Montréal, QC, Canada, ⁵Laboratoire de Suivi Thérapeutique Pharmacologique et Pharmacocinétique, Faculté de Pharmacie, Université de Montréal, Montréal, QC, Canada, ⁶Centre de Recherche, CHU Sainte-Justine, Montréal, QC, Canada

PURPOSE: Rifampicin (RIF) is a pivotal antibiotic in tuberculosis treatment. However, its pharmacokinetic varies greatly between subjects. This can lead to low RIF concentrations, which is associated with therapy failure and acquired drug resistance¹. Population pharmacokinetic (PopPK) models can help predict a patient's antibiotic concentration. This study aimed to conduct external evaluations of the published RIF PopPK models.

METHOD: Published RIF's PopPK models were identified in a PubMed search. Clinical data and RIF blood concentrations were retrospectively collected from adult tuberculosis patients treated with oral RIF and followed at the Assistance Publique des Hôpitaux de Marseille (France). Using the software NONMEM (Icon Development, v7.5), *a priori* and *a posteriori* predictions were estimated at each sampling time. Prediction errors, the difference between measured and predicted RIF concentration, were calculated. Model predictive performances, composed of both bias, the median of prediction errors, and imprecision, the median of absolute values of prediction errors, were evaluated.

RESULTS: From the 199 identified articles, five were selected for external evaluation. A population of 68 patients (111 samples, 32.4% women, median age of 37.5 years) was studied. All models had imprecision or bias for *a priori* predictions above their 30% and $\pm 20\%$ respective cutoff. Parameters of the model with the lowest *a priori* predictions' bias and imprecision (17.9% and 40.8% respectively) were re-estimated to fit the population. It decreased the value of the volume of distribution, diminished the *a priori* predictions' bias to 6.4%, but did not improve imprecision, resting at 44.2%.

CONCLUSION: No original or re-estimated models had an acceptable predictive performance. Weight, a key co-variable in RIF's PopPK models, was not available in the population, potentially leading to a

selection of more population-specific models, and thus, to higher imprecision. This study highlights the importance of conducting external validations to ensure the reliability of PopPK models.

References

J Infect Dis. 2013 Nov 1;208(9): 1464-73

Developing a Pharmacy-Specific Suicide-Prevention Program for E2P PharmD Students

Wen Liao

University of British Columbia

Background: Suicide has been an ongoing health crisis in Canada. However, they are preventable, especially when warning signs of suicide are identified early on. As frontline healthcare providers, pharmacists can play a critical role in assisting patients at risk of suicide. Many Canadian pharmacists, however, feel under-equipped to do so. Although several well-established suicide-training programs exist, none of them has been tailored to address the needs of pharmacists during their daily interaction with patients.

Objective: We aim to develop the first pharmacy-specific suicide prevention training in Canada to address the knowledge gap pharmacists face daily in their practice.

Hypothesis: We hypothesize that with the implementation of the pharmacy-specific suicide training program, graduates from the UBC PharmD program will feel prepared when encountering patients who might be at risk of suicide.

Methods: A literature review was performed to scan for currently available suicide-prevention training. Selected works of literature and training programs were carefully reviewed and compared. Several key areas were evaluated, including learning objectives, modes of delivery, target audiences, and durations of training. Training contents were

examined for their suitability in a Canadian healthcare context.

Result: We developed a two-part, mixed-delivery suicide-prevention training program that can be integrated into the Psychiatry module of the UBC E2P PharmD program. The asynchronous portion is didactic, providing factual information about suicide and its relevance in Canada. The synchronous portion is interactive, where the students practice and apply suicide-prevention skills acquired in the asynchronous part via role-playing, video scenarios, and self-reflection.

Conclusion: This program represents the first pharmacy-specific suicide-prevention training to be implemented in a Canadian PharmD program. Through this training, students will be able to identify warning signs and initiate a conversation about suicide with patients. This program encourages conversations around suicide, reduces mental health stigma, and improves patient-care quality.

Three-Dimensional-Printed Alginate/Gelatin Patches for Cardiac Tissue Engineering Applications

Farinaz Ketabat¹, Titouan Maris², Xiaoman Duan¹, Zahra Yazdanpanah¹, Michael Kelly³, Xiongbiao Chen¹, Ildiko Badea⁴

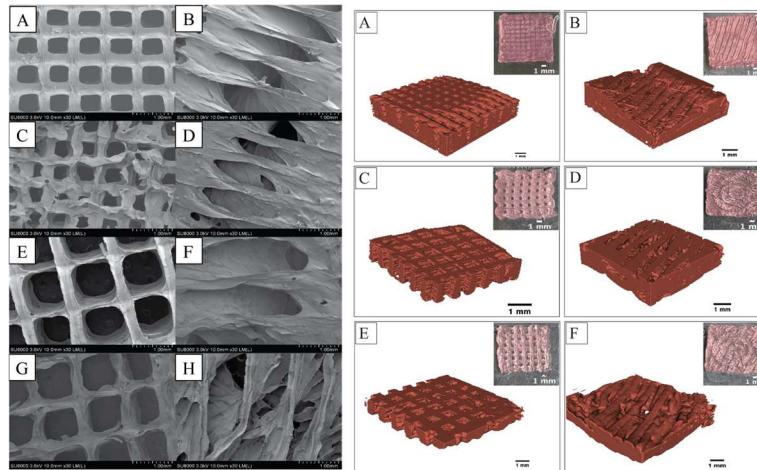
¹Division of Biomedical Engineering, University of Saskatchewan, SK, Canada, ²Institut Catholique des arts et métiers (ICAM)- Site de Toulouse, France, ³Department of Surgery, College of Medicine, University of Saskatchewan, Saskatoon, Canada, ⁴College of Pharmacy and Nutrition, University of Saskatchewan, Saskatoon, Canada

Purpose: Creating synthetic cardiac tissue that mimics the hierarchical structure of cardiac tissue remains challenging, raising the need for the development of novel methods capable of creating structures with high complexity. Three-dimensional (3D)-printing techniques are among promising additive manufacturing methods for creating complex tissue constructs with high precision. This study aims to create a platform for growing cardiac tissue.

Method: We designed and fabricated 3D patches that mimic the orientation of heart fibers (angular structures) using alginate (Alg) and gelatin (Gel) as well as two cell types, including human umbilical endothelial cells (HUVECs) and H9c2 cells. The 3D-printed structures were characterized in terms of morphological evaluations via scanning electron microscopy (SEM) and synchrotron radiation propagation-based imaging computed tomography (SR-PBI-CT), physical characteristics, including elastic modulus, swelling ratio, and mass loss rate. The cell viability studies via measuring the metabolic activity of the live cells with MTT assay and visualizing the cells with live/dead assay kit.

Results: The composites of Alg and Gel at ratios of 2 to 1 and 3 to 1 (Alg2Gel1 and Alg3Gel1) showed the highest cell survival; they accordingly were used to fabricate two different structures including angular and lattice. Scaffolds made of Alg3Gel1 showed higher elastic modulus, lower swelling rate percentage, less mass loss, and higher cell survival compared to that of Alg2Gel1. Patches fabricated from Alg3Gel1 with infill distance of 1.5 mm and strand diameter of 0.15 mm (Alg3Gel1[1.5,0.15]-A) showed the highest cell viability with better mechanical and physical properties compared to the other investigated groups.

Conclusion: The 3D-printed structures made of Alg3Gel1[1.5,0.15]-A have illustrated promising results for cardiac tissue engineering by providing high cell viability for both endothelial and cardiac cells, high mechanical strength, and appropriate swelling as well as mass loss properties during 21 days of incubation at physiological condition.



Effect of Exercise on Cerebral Inflammation in a Pre-Eclampsia Mouse Model

Noriko Daneshtalab¹, Martin Dimitrov²

¹Supervisor, ²Author

Introduction:

Preeclampsia (PE) is a disorder of pregnancy characterized by increases in blood pressure (BP) due to increases in sensitivity to vasoconstrictors including the products of the Renin-Angiotensin Aldosterone System (RAAS). Increases in BP can lead to neuroinflammation, and it has been demonstrated that exercise decreases BP. It is theorized that exercise could decrease neuroinflammation in preeclamptic patients. This neuroinflammation can be quantified through the measurement of inflammatory cell regulation.

Materials & Methods: *Animal Models:* Pregnancy Superimposed on Chronic Hypertension (PESCH) mouse models were placed into groups based on baseline characteristics such as pregnancy, hypertension, exercise trained, and treatment with MAS-receptor agonist.

Methods: Fixed brain samples (sent from University of Montreal) were blocked and cut at 5uM on slides. Samples were deparaffinized using standard procedures and incubated with primary antibodies, GFAP-Cy3

(1:1000), Iba1 (1:1000), and DAPI (1:1000), Iba1 was further labelled with the secondary antibody GAR- Cy5 (1:200). The hippocampus, hypothalamus, and cortex were then imaged using Zeiss LSM-900 confocal microscope and analyzed using ImageJ.

Results & Discussion:

Quantitative analysis of mean grey value (correlating to astrocyte spread) showed differences in astrocyte spread in hypertensive vs. normotensive groups. MAS-receptor agonist treatment also appeared to affect astrocyte spread in the hypothalamus and dentate gyrus (DG). A significant decrease in both Type 1 and Type 2 microglial cell count was observed within the hippocampus and hypothalamus with MAS-receptor treatment.

Conclusion:

Current analysis appears to indicate altered astrocyte expression due to hypertension and pregnancy. The data also indicates treatment with MAS receptor agonist decreases microglial expression for sedentary and pregnant groups that indicates a potential role for anti-inflammatory effect in the brain with the activating Mas receptor. Further research in the role of microglia in the specific brain regions during hypertension and pregnancy is needed.

Development of Pimozide-loaded Liposomal System for the Treatment of Type 2 Diabetes

Sirazum Munira¹, Seyed Amirhossein Tabatabaei Dakhili¹, Christina T. Saed¹, John R. Ussher¹, Afsaneh Lavasanifar¹

¹Faculty of Pharmacy and Pharmaceutical Sciences, University of Alberta

Purpose: Elevated skeletal muscle succinyl CoA:3-ketoacid CoA transferase (SCOT) activity, the rate-limiting enzyme of ketone body oxidation, was observed to contribute to obesity and type 2 diabetes (T2D) associated hyperglycemia. Of interest, a recent study observed that the diphenylbutylpiperidine pimozide (PMZ), which is an older generation antipsychotic agent, is capable of inhibiting SCOT and

decreasing ketone oxidation. Moreover, obesity-induced hyperglycemia in mice was reversed by treatment with PMZ. However, it is critical that pimozide avoids crossing the blood-brain barrier (BBB) in order to prevent its CNS-related side effects (e.g. dizziness, dyskinesias). Liposomes with PEG-conjugated lipids in their outer layer are promising nano-carriers for both hydrophilic and hydrophobic compounds and are known to avoid crossing BBB. This research aims to develop a PMZ-loaded liposomal system as a means of limiting the brain permeability of this drug.

Method: The mixture of lipids DSPC, cholesterol, DSPE-PEG2000 lipids and PMZ dissolved in appropriate organic solvents were evaporated to prepare a thin film in a round-bottom flask. The lipid film was hydrated with citrate buffer (pH 3.5). The unloaded PMZ was separated from the PMZ-loaded liposome and the acidic buffer was exchanged by washing with purified water in a size-exclusion chromatography column. The developed formulations were characterized for their encapsulation efficiency, in vitro drug release, size and morphology. In addition, the SCOT activity of free PMZ and its liposomal formulation in the C2C12 mouse myoblast cell line following treatment was evaluated by quantification of the rate of acetoacetyl-CoA production using a UV-Vis spectrophotometer.

Results: The liposomal formulation of PMZ showed an encapsulation efficiency of 63%, and an average diameter of 93 nm. In vitro release study showed a slower release of PMZ-liposome (71.2%) than the free PMZ over 24 hours.

Conclusion: Encapsulating PMZ within liposomes improves the release profile of loaded drugs.

Hypoxic placenta on a chip as a model of preeclampsia for the evaluation of CSA-coated liposomes

Luis A Perez Davalos¹, Jack Tyrrell¹, Amr Abostait^{1, 2}, Mahmoud Abdelkarim^{1, 3}, Hagar Labouta^{1, 2, 3, 4}

¹College of Pharmacy, University of Manitoba, Winnipeg R3E 0T5, Canada , ²Children's Hospital Research Institute of Manitoba, Winnipeg R3E 3P4, Canada , ³Biomedical Engineering, University of Manitoba, Winnipeg R3T 5V6, Canada , ⁴Faculty of Pharmacy, Alexandria University, Alexandria 21521, Egypt

PURPOSE

Preeclampsia is a hypertensive disorder of pregnancy that can impact severely maternal and fetal health. It is the second leading cause of maternal mortality worldwide, and the incidence rates keep rising¹. Unfortunately, current treatments solely prevent complications and fail to address the underlying mechanisms of the disease. The complex pathogenesis and the inaccuracy of standard preclinical models hinder the clinical translation of novel therapies. Chondroitin sulfate A (CSA)-coated liposomes have been proposed as effective nanocarriers for targeted delivery to the placenta². Hence, this work aims to develop a hypoxic placenta-on-a-chip model that recapitulates the local microenvironment in preeclampsia for the in vitro assessment of CSA-functionalized liposomal nanocarriers.

METHODS

Using microfluidics chips, BeWo b30 cells were cultured to assess syncytialization in response to shear stress and forskolin, compared to static cell cultures. Cobaltous chloride was added to mimic the trophoblasts' response to hypoxia, as observed in preeclampsia. Cell viability and hypoxia-inducible factor 1 α (HIF-1 α) expression were assessed under dynamic and static conditions. Furthermore, this model was used to assess the cytotoxicity and uptake of CSA-coated liposomes that were prepared using microfluidics synthesis.

RESULTS

Increased syncytialization and microvilli formation were observed in dynamic cultures even in the absence of forskolin, suggesting that shear stress is determinant for placental development. No significant cytotoxicity was observed on liposome-treated cells compared to non-treated cells. Higher cellular uptake was observed under dynamic vs static conditions, and CSA coating enhanced liposome uptake.

CONCLUSION

This hypoxic placenta on a chip is a biologically relevant model of preeclampsia for the evaluation of novel targeted nanomedicine therapeutics. CSA-coating improved the uptake of liposomes, which can be applied as suitable nanocarriers for targeted delivery to the placenta to treat maternal-fetal diseases such as preeclampsia. Furthermore, this model will be used to understand better the pathogenesis of the disease.

References

1. Say, L., Chou, D., Gemmill, A., Tunçalp, Ö., Moller, A. B., Daniels, J., Gülmezoglu, A. M., Temmerman, M., & Alkema, L. (2014). Global causes of maternal death: a WHO systematic analysis. *The Lancet. Global health*, 2(6), e323-e333. DOI: 10.1016/S2214-109X(14)70227-X
2. Li L, Yang H, Chen P, Xin T, Zhou Q, Wei D, Zhang Y, Wang S. Trophoblast-Targeted Nanomedicine Modulates Placental sFLT1 for Preeclampsia Treatment. *Front Bioeng Biotechnol*. 2020 Feb 11;8:64. doi: 10.3389/fbioe.2020.00064. PMID: 32117942; PMCID: PMC7026029.

Synthesis and evaluation of IT3S3 as a therapeutic against *Clostridioides difficile* toxin

Rebecca Cummer¹, Raphaël Bolteau¹, Jean-François Trempe¹, Bastien Castagner¹, Lauren Finn², Bettina Keller²

¹McGill University, Montreal, QC, ²Freie Universität Berlin, Berlin, Germany

Purpose: *Clostridioides difficile* (*C. diff*) is a bacterium that causes the most prevalent form of hospital-acquired infection. *C. diff* infection (CDI) is caused by antibiotics as they disrupt the gut microbiota that prevents *C. diff* from colonizing, resulting in high rates of disease relapse. Consequently, there is a need for new treatments against CDI. One treatment strategy would be to target toxins released by *C. diff*. The toxins make an ideal drug target as they are the primary cause of symptoms.

Method: We previously published an approach to target the toxins using analogues of inositol hexakisphosphate (IP6). IP6 is a natural co-factor of the toxin's cysteine protease domain (CPD), responsible for triggering the auto-processing of *C. diff* toxins in enterocytes. Our analogues preemptively induce toxin cleavage, neutralizing them before they enter enterocytes. We have synthesized new IP6 analogues to further explore their structure-activity-relationship with the toxin. First, we determined the ability of the IP6 analogues to cleave the holotoxin *in vitro*. Second, we used isothermal calorimetry to quantify the dissociation constants of the compounds with the CPD. Next, we performed a thermal shift assay to determine the stability of the toxin/analogue complexes. Finally, docking studies were conducted to explore their binding pose in the CPD.

Results: A new IP6 analogue, IT3S3, significantly improved holotoxin cleavage compared to IP6 ($p < 0.01$). IT3S3 had a decreased dissociation constant ($K_{d,IP6} = 1.36M$, $K_{d,IT3S3} = 500nM$) and improved CPD stability compared to IP6 ($T_{M,IP6} = 60.8^{\circ}C$, $T_{M,IT3S3} = 63.6^{\circ}C$). Finally, IT3S3 and IP6 maintained alternative binding poses in the CPD.

Conclusion: IT3S3's decreased dissociation constant improved its ability to cleave holotoxin in comparison with IP6. This was not observed with our previous lead compound, IT2S4. By enhancing toxin cleavage, we anticipate IT3S3 will outperform IT2S4 when tested in a fulminant mouse CDI model.

References. Yonsei Med J 2018 59: 4-12. Cell Chem Biol 2019 26: 17-26

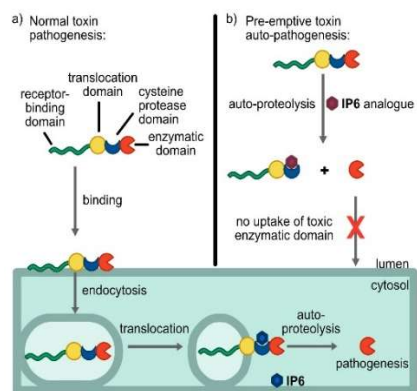


Figure 1. a) Pathogenesis of *C. difficile* toxin. b) Scheme of drug design tactic.

Nanoparticle T-cell engagers for local combination therapies

Ryan Wylie, Kevin Wai

McMaster University

Purpose: Bi-specific T-cell engagers (BiTEs) have shown remarkable antitumor properties due to their ability to redirect cytolytic activity of T-cells via CD3 binding towards cancer cells. However, they have limitations due to their short plasma half-life and the dependence on the expression of a single tumor associated antigen (TAA). Multi-antigen T-cell engagers (MATEs) are BiTE-like therapeutics being developed and optimized for local delivery to target multiple antigens simultaneously and avoid systemic clearance and toxicity. The MATE design utilizes nanoparticles that may also encapsulate small molecule drugs to be modified with TAA and CD3 targeting antibodies. The design incorporates local delivery of small molecules with the immunotherapeutic benefits of T-cell engagers.

Methods: To screen the influence of antibody grafting density and nanoparticle size, carboxylic acid coated polystyrene nanoparticles were modified with TAA and anti-CD3 antibodies. To evaluate anti-HER2 modified MATE bioactivity, T-cell mediated cytotoxicity assays were performed with different cancer and healthy cell-lines: HER2+ human breast cancer cells (SK-BR-3), and a HER2- immortalized human embryonic kidney cells (HEK293).

Results: Preliminary experiments using anti-CD3 and anti-HER2 modified MATEs have shown effective killing of the HER2+ SK-BR-3 cancer cells in the presence of T-cells, indicating the effective bridging of T-cells with the cancer cells for T-cell mediated cytotoxicity. The MATE format also shows specificity to only kill HER2+ SK-BR-3 by displaying non-significant neutralization of the HER2- HEK293 cells. Current *in vitro* experiments using 100, 200, and 500 nm particle sizes suggests cytotoxicity is independent of particle size. Significant cytotoxicity is seen at anti-CD3 antibody densities as low as ~4 antibodies per nanoparticle.

Conclusions: The targeted killing of HER2+ cancer cells were confirmed with anti-HER2 MATEs. We are now evaluating CD133 targeting MATEs for the targeting of multiple TAAs and exploring PLGA nanoparticles in lieu of polystyrene for combination therapies with small molecules.

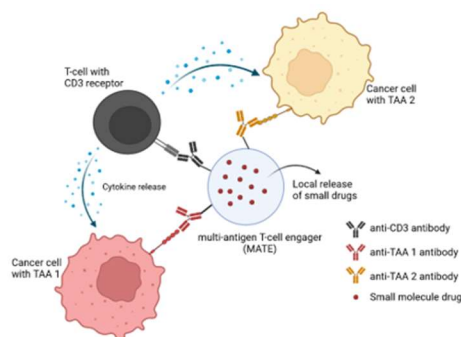


Figure 1: Multiple TAA targeting antibodies and CD3 targeting antibodies are modified onto a nanoparticle scaffold to function as a BiTE-like therapeutic. The nanoparticle will also be encapsulated with small molecule drugs to also function as a local delivery of cancer killing small molecules.

Tunable mucoadhesion and mucopenetration using self-assembled brush-block copolymer-based nanoparticles.

Ridhdhi Dave¹, Andrew Singh¹, Cecile Fradin¹, Francisco Goycoolea², Heather Sheardown¹, Todd Hoare¹

¹McMaster University, ²University of Leeds

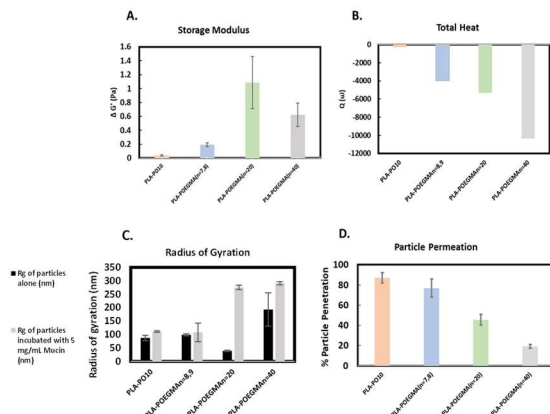
Purpose: Self-assembled nanoparticles

(NPs) are promising drug delivery vehicles to the eye. However, current methods often use poly(ethylene glycol) (PEG), which has limited chemical functionality and poor mucosal adhesion and penetration^{1,2}. Herein, we created self-assembled NPs from poly(oligo (ethylene glycol) methacrylate) (POEGMA), a brush polymer derivative of PEG, and poly(lactic acid) (PLA) to offer easy functionalization via free radical copolymerization while facilitating tunable molecular weights³. We hypothesize that controlling the PEG sidechain length in the POEGMA brush can control mucopenetration/mucoadhesion.

Methods: NPs were prepared through self-assembly of PLA and POEGMA-based amphiphilic block-copolymers. POEGMA_n blocks were polymerized to different chain lengths using OEGMA monomers (n=2-40). NPs were self-assembled using flash nanoprecipitation and characterized for size (DLS) and morphology (TEM). Mucoadhesion was validated between NP and mucin using (1) rheological synergism experiments, (2) asymmetrical field-flow fractionation to determine the formation of a protein corona, (3) isothermal titration calorimetry to determine total heat flux, and (4) fluorescence quenching to measure binding constants. Mucopenetration is measured by (1) particle diffusion studies and (2) through single particle tracking.

Results: Amphiphilic block-copolymers were polymerized to different POEGMA chain lengths with Mn of ~25 kDa. Small (<250 nm) and monodisperse (PD <0.2) NPs were synthesized. NPs fabricated from long amphiphilic block-copolymers (PLA-POEGMA_{n=20,40}) demonstrated mucoadhesion through an (Fig.A) increase in storage (G') modulus when mixed with mucin, (Fig.B) higher total heat flux generated from NP-mucin interactions, and (Fig.C) formation of larger NP-mucin hybrid structures indicated through increases hydration radius. Comparatively, NPs fabricated with the short chain polymers (PLA-PO10 and PLA-POEGMA_{n=8,9}) were able to penetrate through the mucin layer at high permeation rates (>80%) in comparison to their long chain analogs (Fig.D).

Conclusion: NPs self-assembled from PLA-POEGMA block-copolymers can mimic the favorable properties of PEG-based NPs to enable mucosal penetration and adhesion for accessing the front of the eye.



References

1. C. Lynch, *Polymers (Basel)*, 11 (2019) 1371.
2. M. Rafat, *Biomaterials*, 31 (2010) 3414-3421.
3. Q. Xu, *ACS Nano*, 9 (2015) 9217-9227.

In Vitro Cancer Model for Monocyte Migration using iFlowPlate™

Mandeep Marway
McMaster University

Introduction: Monocytes recruited from the bone marrow to the tumor site differentiate into tumor-associated macrophages (TAMs) and play a key role in tumor progression and metastasis¹. Screening of monocyte-targeting therapies to prevent recruitment or differentiation to TAMs may hinder tumor progression and improve therapies. We are developing an *in vitro* screening tool to characterize monocyte infiltration across an endothelial barrier, through extracellular matrix environments towards embedded cancer spheroids (Figure 1A). The iFlowPlate™ technology is a high-throughput screening platform, created on a 384-well plate containing 128 perfusable networks, each created by connecting 3 adjacent wells using a single channel² allowing for the screening of drug combinations and sustained release drug delivery vehicles.

Methods: Glioblastoma (BT935) spheroids were embedded within fibrin hydrogels with a confluent layer of human umbilical vein endothelial cells (HUVECs) on the gel surface. Barrier function was confirmed by quantifying the diffusion of 4 and 65 kDa dextran. Finally, monocytes were introduced above the barrier and migration was monitored by confocal microscopy.

Results: HUVECs consistently formed confluent monolayers within 5 days of seeding at 2×10^5 cells/mL on fibrin gel surfaces. The barrier function and basal membrane were confirmed using dextran permeability and immunohistochemistry. The model is now being used to follow the real-time migration of monocytes under various conditions. For example, monocyte migration was only observed in the presence of cancer spheroids (Figure 1B), indicating signalling pathways that encourage monocyte migration were established. We are now conducting cytokine release assays to identify chemotactic agents. Drug and delivery vehicle screening will be performed to inhibit and promote monocyte recruitment and differentiation.

Impact: The recruitment and differentiation of monocytes to TAMs in the tumor environment is an important question for drug screening. The iFlowPlate™ allows for visualizing monocyte recruitment, and screening for drugs to prevent recruitment and differentiation to TAMs.

References

- 1) Cancer Microenviron 2013 6(2): 179-191
- 2) Adv. Mater. 2020 32(46): 2002974

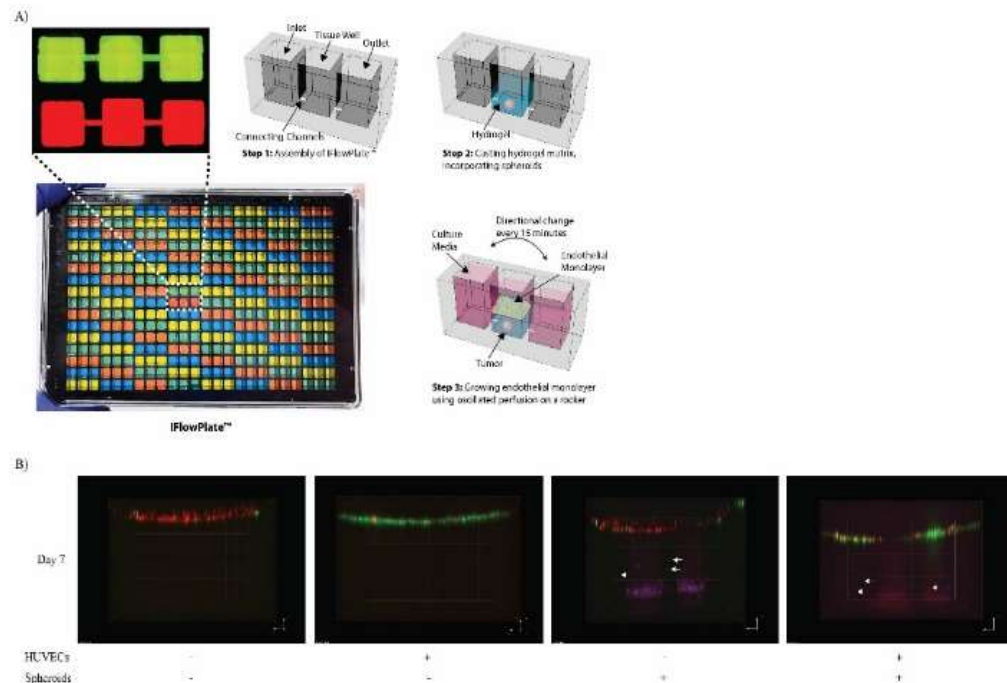


Figure 1: A) iFlowPlate™ is a 384-well plate composed of 128 perfusable networks, each made of 3 wells connected by 2 channels. Spheroids are embedded in a fibrin hydrogel and a HUVEC monolayer is grown on the surface. The HUVEC monolayer (green) becomes confluent after 5 days. B) Monocyte (red) migration is only seen when spheroids (purple) are present. The migrating monocytes are indicated with an arrow. The conditions in which there are no spheroids, the monocytes remain at the surface of the gel.

The Impact of Static Pressure on Trophoblast Cellular and RNA-Level Responses in a Placenta-on-a-chip model

Mahmoud Abdelkarim^{1, 2, 3}, Yasmin Abdelkader^{2, 3}, Hagar I. Labouta^{1, 2, 3, 4, 5}

¹Biomedical Engineering, University of Manitoba, Winnipeg, Manitoba, R3T 5V6, Canada., ²College of Pharmacy, University of Manitoba, Winnipeg, Manitoba, R3E 0T5, Canada., ³Keenan Research Centre for Biomedical Science of St. Michael's Hospital, Unity Health Toronto, University of Toronto, Toronto, ON M5B 1T8, Canada, ⁴Children's Hospital Research Institute of Manitoba, Winnipeg, Manitoba, R3E 3P4, Canada., ⁵Leslie Dan Faculty of Pharmacy, University of Toronto, 144 College Street, Toronto, ON, M5S 3M2, Canada

Purpose: The placenta is a biological barrier that supports the growth and maturation of the fetus and undergoes many structural changes as pregnancy progresses. The mechanical microenvironment, mainly shear stress on the cells, influences barrier formation by activating many

signalling pathways through mechanotransduction mechanisms [1,2]. However, the impact of static pressure on the placental barrier is overlooked. We hypothesize that changing the static pressure exerted on the trophoblasts under dynamic fluid flow will trigger changes in the cellular responses and gene expression levels.

Method: BeWo cells were cultured in tissue culture-treated microfluidic channels, iBidi μ -Slide I^{0.4}. Different pressure conditions were studied for 24 hours (high pressure= 20 kPa, low pressure= 200 Pa) under dynamic conditions versus control static conditions (P=0). Flow rate and shear stress were kept constant at 2 μ l/min and 0.0025 dyne/cm², respectively. The three models were evaluated for syncytial formation by β -hCG secretion, and RNA expression was measured by real-time PCR.

Results: We observed higher cell adherence and the formation of more syncytia under high-pressure conditions. In addition, as a preliminary result, we found differences in the expression level of genes related to shear stress, heat shock proteins and cell adhesion. Moreover, a difference in the secretion of (β -hCG) was detected between high and low pressure conditions. Ongoing work is being done further to characterize the RNA and protein responses using omics approaches.

Conclusion: Trophoblasts are able to sense fluid shear stress and changes in pressure, which activates multiple signalling pathways. Therefore, it was necessary to consider the pressure values used in the hydraulic circuit to simulate the microenvironment surrounding the cells. These findings help direct future research to reduce the discrepancies due to the variation in pressure values among different studies and to develop models that better mimic the microenvironment.

References

1. Molecular Pharmaceutics 19, 3757-3769 (2022).
2. Expert opinion on drug delivery 20, 13-30 (2023).

Size-dependent internalization of liposomes in cancer spheroid-on-a-chip microfluidic model

Ilya Yakavets¹, Monica Ayachit², Sina Kheiri¹, Faeze Rakhshani¹,
Samantha McWhirter¹, Gilbert C. Walker¹, Edmond W.K. Young¹, Eugenia
Kumacheva¹

¹University of Toronto, Toronto, ON, ²Queen's University, Kingston, ON

Purpose: Nanomedicine has the potential to improve the biodistribution of encapsulated compounds by delivering them selectively to the pathological site and/or avoiding exposure of potentially endangered tissues (site-avoidance drug delivery) [1]. To improve the prediction of the performance of nanoparticles (NPs) within the human body, the development of preclinical in vitro tumor models to represent the complex processes of NPs transport under close-to-physiological flow is of great importance.

Methods. Fluorescently-labelled liposomes with different dimensions were generated by employing microfluidics (MF) and supplied to cell-free microgels and breast cancer spheroids in an MF spheroid-on-a-chip platform. Breast cancer spheroids were grown in tissue-mimetic hydrogel using breast carcinoma MCF-7 cells [2]. Spheroids grew under near physiological flow conditions for 24 hours and were then subjected to liposome formulations with various sizes by continuous perfusion for 2 days. Uptake and retention kinetics of liposomes in individual cell-free microgels and spheroids were examined using wide-field fluorescence microscopy. The penetration of liposomes was assessed using confocal fluorescence microscopy after 2 days of incubation.

Results. We generated arrays of biomimetic microgels and breast cancer spheroids with a uniform size of 300 μm using an MF spheroid-on-a-chip platform. We explored the effect of bidirectional flow on the accumulation, retention and penetration of liposomes with dimensions of 42, 92, 131, and 197 nm in cell-free biomimetic microgels and breast cancer spheroids. We distinguished the role of advection and diffusion in the transport of liposomes of various sizes to microgels and cancer spheroids.

Conclusion: We developed an innovative MF spheroid-on-a-chip platform utilizing a biomimetic hydrogel matrix, uniformly sized spheroids, and spheroid growth under near physiological flow. The platform can be used for the screening of nanomaterials for a wide range of applications, including cosmetics and vaccine development.

References

Nat Rev Drug Discov 2021 20: 101-124

Nat Commun 2022 13: 1466

Protective Effects of Pyrroloquinoline Quinone in a Folate-Deficient Model of the Human Blood-Brain Barrier

Vishal Sangha, Sara Abdoulhassane, Reina Bendayan

Leslie Dan Faculty of Pharmacy, University of Toronto

Purpose: Folates (Vitamin B9) are critical for normal growth and development, with uptake mediated by three major transport systems: folate receptor alpha (FR α), proton-coupled folate transporter (PCFT), and reduced folate carrier (RFC)¹. In the brain, cerebral folate uptake primarily occurs at the blood-cerebrospinal fluid barrier (BCSFB) through coordinated actions of FR α and PCFT, with impairments in this transport resulting in the pediatric neurological disorder cerebral folate deficiency (CFD)¹. To identify novel treatment strategies for CFD, we have identified the induction of RFC by nuclear respiratory factor 1 (NRF-1) at the blood-brain barrier (BBB), once activated by the natural compound pyrroloquinoline quinone (PQQ)¹. PQQ is also of interest due to its anti-inflammatory, antioxidant, and mitochondrial biogenesis effects². In this study, we examined the role of folate deficiency in inducing BBB dysfunction, with PQQ's role in reversing these effects.

Methods: Immortalized human brain microvessel endothelial cells (hCMEC/D3) grown in a folate-complete media (control) or media lacking folic acid [folate-deficient (FD) condition] were treated with 1 or 5 μ m PQQ (or DMSO vehicle) for 24 hours. Following treatment, cells were collected for qPCR analysis to examine changes in gene expression of several tight junction associated proteins, and the folate transport systems.

Results: Gene expression of the tight junction associated proteins occludin and ZO-1, and the folate transporter PCFT were significantly decreased in FD conditions, with claudin-5 expression increased compared to control. PQQ treatment led to significant increases in gene expression of occludin, ZO-1 and PCFT compared to control.

Conclusion: These results demonstrate the effects of folate deficiency in inducing BBB dysfunction, which may contribute to the neurological deficits observed in CFD. PQQ may represent a novel treatment strategy

for disorders associated with CFD, as it can increase folate uptake, while in parallel restoring BBB function. (*Supported by NSERC*).

References

- [1] Trends Pharmacol. Sci. 2020 41: 349-361
- [2] Biosci. Biotechnol. Biochem. 2016 80: 13-22

Lipid Nanoparticles for Fetal Lung Delivery of microRNA-200b: In vitro and ex-vivo assessment.

Amr Abostait¹, Wai Hei Tse¹, Yuichiro Miyake¹, Jackie Wang¹, Arzu Aptekmann¹, Richard Keijzer¹, Hagar Labouta¹

¹University of Manitoba, Winnipeg, MB.

Introduction:

Congenital diaphragmatic hernia (CDH) is a deadly abnormality of the fetal lungs with no cure. Micro-RNA-200b showed promising results in restoring normal lung development and decreasing the incidence of CDH[1]. To deliver microRNA-200b safely and specifically to the fetal lung during pregnancy, it requires a carrier. We aim to encapsulate it inside targeted lipid nanoparticles (LNPs) and evaluate two injection routes, local injection to the fetal lung and maternal intravenous (i.v) injection.

Methods:

We used microfluidics to synthesize a library of LNPs varying in ionizable lipids, PEGylated lipids, and cationic lipid percentage. To design formulations with different antibody (Ab) orientations, lipids with different end-functional groups were incorporated into the LNPs composition. All LNPs were characterized for physicochemical properties. LNPs intended for the i.v. route were evaluated in a placenta-on-a-chip model of BeWo placental cells and human umbilical vein endothelial cells (HUVEC), before preclinical testing in a rat model of CDH. The local injection route was evaluated using an ex-vivo E18 fetal lung explant.

Results

Microfluidics enabled the formation of stable monodisperse LNPs with

reproducible physicochemical parameters. The number of Abs per LNP was in the range of 4-20 for the different formulations and Ab orientations as determined by nanoparticle tracking analysis. The distance between individual Abs on the LNP surface ranged from 84-39nm. Dynamic flow, in the placenta-on-a-chip model, induced different cell morphologies and receptors expression. All LNPs were not toxic in vitro, using calcein and ViaLight assays, and ex vivo using H&E staining.

Conclusion

We are evaluating two novel approaches for fetal delivery using Ab-functionalized LNPs. Nanoparticle tracking analysis enables quantifying the Ab density on the LNP surface, which facilitates the mechanistic understanding of Ab-based targeting of LNPs. Further, the placenta-on-chip model is more representative of the placental microphysiology, and enables preclinical evaluation of LNPs under biomimetic conditions.

References

[1] Annals of Surgery 269(5):p 979-987, May 2019.

Testing of liposomal blood lactate assay with portable fluorometer in human blood

Simon Matoori¹, Natalie Guirguis¹, Arturo Israel Machuca-Parra¹

¹Université de Montréal

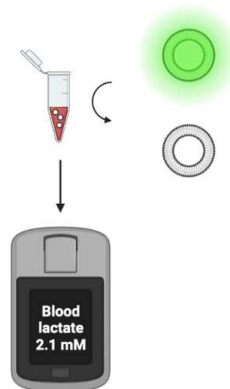
Introduction. In sepsis, plasma lactate is a widely used biomarker for disease staging and assessment of treatment success. In clinical practice, lactate testing is conducted in the hospital laboratory and leads to a time loss of three hours. To shorten the time to result, we developed a bedside blood lactate assay (Figure 1, Matoori & Mooney, Small 2020; Biomaterials 2022). This liposomal assay is based on a two-step enzymatic reaction inside a vesicular reaction compartment where lactate is oxidized by lactate oxidase. The hydrogen peroxide generated in this reaction is used by horseradish peroxidase to oxidize and quench the near-infrared fluorescent dye sulfo-cyanine 7. We successfully showed the performance of this test in human blood using a conventional

tabletop fluorometer. Here, we are combining the liposomal assay with a small portable fluorometer that enables bedside testing.

Methods. The fluorescence intensity of sulfo-cyanine 7 was measured at pH 7.4 using the portable fluorometer (Deniro, Detact Diagnostics). Liposomes loaded with sulfo-cyanine 7, lactate oxidase, and horseradish peroxidase were prepared. The liposomes were incubated with lactate-spiked commercial whole blood and the fluorescence intensity was measured over five minutes.

Results. At pH 7.4, the fluorescence intensity was highly linear in the range of 8 to 2000 nM ($R^2 = 0.992$). In lactate-spiked human blood, the liposomal assay showed a linear response to lactate in a range of at least 0.6 to 5 mM after two minutes ($R^2 = 0.974$). This response covers the clinically used cut-off in sepsis (2 mM).

Conclusion/Implications. We are developing a rapid, and easy-to-use bedside assay for blood lactate measurements. In this study, we combined the lactate assay with a portable fluorometer and observed fast and linear lactate sensing in human blood. This lactate assay promises to provide a new point-of-care option for sepsis diagnostics and assessment of treatment response.



References

- [1] LW Andersen et al. Mayo Clin Proc. 2013; 88:1127-1140
- [2] M Goyal et al. J Emerg Med 2010; 38:578-581

The Cellular Sources of Amyloid-Induced IL-1 β Production in Pancreatic Human Islets - Implications for New Pharmacological Strategies in Type 2 Diabetes

Danish Malhotra, Lucy Marzban

College of Pharmacy, University of Manitoba

Purpose. Formation of β -cell toxic protein aggregates named islet amyloid is a pathologic characteristic of the pancreatic islets in type 2 diabetes (T2D), which also occurs in human islets during pre-transplant culture and post-transplantation. Islet amyloid is mainly comprised of a normally produced β -cell hormone, human islet amyloid polypeptide (hIAPP; amylin), which is co-secreted along with insulin from β -cells. The mechanisms by which amyloid formation destroys β -cells are still unclear. We previously showed that amyloid formation promotes islet interleukin (IL)-1 β production, resulting in β -cell upregulation of the Fas cell death receptor and apoptosis. Here, we investigated the potential cellular source(s) of IL-1 β production in human islets during amyloid formation *ex vivo*.

Methods. Isolated human islets ($n = 5$; cadaveric pancreatic donors), were treated with or without clodronate (to deplete macrophages) and cultured in elevated (11.1 mmol/l) glucose (to potentiate amyloid formation) for up to 7 days. Paraffin-embedded islet sections were used for quantitative immunolabeling for insulin and each IL-1 β , Fas, TUNEL (to detect apoptosis), thioflavin S (to detect amyloid), and CD68 (macrophage marker).

Results. Freshly isolated human islets had low levels of IL-1 β immunoreactivity. Islet culture in elevated glucose resulted in progressive amyloid formation which was associated with increased islet IL-1 β immunoreactivity (mainly in β -cells), and β -cell Fas upregulation and apoptosis, all of which were prevented by inhibition of amyloid formation. Islet resident macrophages were present in 7-day cultured human islets. Macrophage depletion markedly reduced, but did not completely block, amyloid-induced IL-1 β immunoreactivity in islet β -cells.

Conclusion. In summary, these data suggest that macrophages (mainly) and β -cells are two cellular sources of amyloid-induced IL-1 β production in human islets, which leads to Fas-mediated β -cell apoptosis. Blocking islet IL-1 β production and/or IL-1 β signaling may provide an effective pharmacological strategy to protect islet β -cells from amyloid toxicity in T2D and islet grafts.

Exploring the microfluidic design space for cross-linked poly(lactide-co-allyl-glycolide) microparticles

Jack Bufton¹, Pauric Bannigan¹, Christine Allen¹

¹University of Toronto

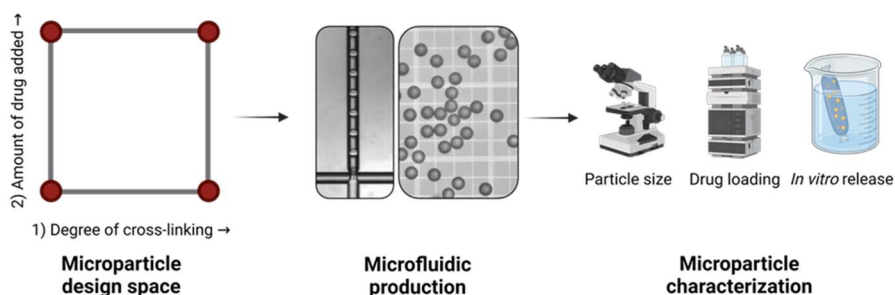
Purpose: Polymeric microparticles (MPs) can provide sustained drug release but are non-trivial to manufacture. Microfluidic manufacturing techniques can facilitate uniform and scalable MP production. However, the multitude of microfluidic processing parameters (e.g., flowrate, fluid composition) form a high-dimensional design space which can influence the physicochemical properties of the resulting MPs (e.g., size, drug loading, *in vitro* release, etc). Quality by design (QbD) principles can allow researchers to better explore the formulation design space in an efficient manner. Our group has previously demonstrated that cross-linked polyester MPs can be used for sustained drug release applications. In this preliminary work, we combine QbD methodology with microfluidic manufacturing to design drug-loaded cross-linked poly(lactide-co-allyl-glycolide) (PLAG) MPs.

Methods: Cross-linked MPs were prepared by exposing reactive PLAG droplets to UV light. Celecoxib was then loaded by immersing the drug and cross-linked MPs in a common organic solvent. A 2² factorial design evaluated the effects of (i) the degree of cross-linking, and (ii) initial drug-to-material ratio on resulting particle size, drug loading, and *in vitro* release.

Results: MPs with an average size of 37-40 μm (<10% relative standard deviation) were produced prior to drug-loading at both cross-linking

ratios. The drug loading was similar for MPs at both cross-linking ratios. Low and high initial drug-to-material ratios resulted in drug loading levels of 4 to 23 wt% with respective encapsulation efficiencies of 80% and 60%.

Conclusions: Initial results indicate MPs with reduced cross-linking have a more rapid *in vitro* release, however, additional studies are warranted. Future work will expand this design space to correlate additional MP properties (e.g., thermal properties) with *in vitro* performance.



Scheme 1: Overview of study workflow. First, the design space of cross-linked microparticles is established. Selected formulations are then manufactured using microfluidic techniques. The grid lines in the image on the right are spaced 50 μm apart. Finally, the microparticles are characterized in terms of size, drug loading and *in vitro* release.

Stereoselective pharmacokinetics of bupivacaine in Sprague-Dawley rats; examination of application of Bayesian forecasting using sparse sampling.

Shamima Parvin, Neal Davies, Dion Brocks

¹University of Alberta, Edmonton, AB

Purpose: To characterize the stereoselective pharmacokinetics of bupivacaine in the rat after subcutaneous (SC) injection, and to explore Bayesian forecasting (BF) as a way to estimate pharmacokinetic parameters (PKP) using sparse sampling.

Methods: Five rats, cannulated at the jugular vein, were given 7.5 mg/kg (\pm)-bupivacaine HCl followed by blood samples for 24 h. Compartmental analysis was used to characterize the model and PKP. In a separate group of rats, 5 mg/kg of bupivacaine HCl was given as SC injection. However, in these rats, two spaced samples per rat were drawn from the

cannula. The PKP were estimated using a Bayesian forecasting program (PKB-est). All plasma samples were assayed for bupivacaine enantiomers using stereospecific LC-MS (lower limit of quantitation 2.5 ng/mL).

Results: Bupivacaine followed a one-compartment model. The C/F, Vd/F, t_{max} and terminal phase half-life for the rich sampling protocol were, for each respective enantiomer: 4.2 ± 0.84 & 4.1 ± 0.76 L/h/kg; 11 ± 5.2 & 11 ± 5.1 L/Kg; 0.87 ± 0.53 & 0.91 ± 0.53 h; and 1.7 ± 0.45 & 1.8 ± 0.48 h, respectively. Using sparse sampling and BF, the corresponding PKP were: 2.7 ± 0.94 & 2.5 ± 0.92 L/h/kg; 11 ± 3.0 & 10.3 ± 2.7 L/kg; 0.74 ± 0.11 & 0.79 ± 0.09 h; and 3.0 ± 0.99 & 3.1 ± 1.2 h, respectively. There were no significant differences noted between the enantiomers when looking at the rich or the sparse sampling data. The only significant difference noted between the data collected from rich and sparse sampling using BF was in CL/F, which was higher for both enantiomers in the rich data set. The rats in those groups were found to differ in body weight ($p < 0.01$, sparse 18% higher than rich sampling group).

Conclusion: The Bayesian method provided estimates of PKP very close to those of rats where rich sampling was done. There was a difference in body weight and age which may have contributed to a difference in CL/F.

The Difference between amyloid-induced Fas expression in islet α -cells and β -cells - Implication in type 2 diabetes and β -cell targeted pharmacotherapy

Mukta Moni, Lucy Marzban

University of Manitoba, Winnipeg, MB

Purpose: Type 2 diabetes (T2D) is characterized by β -cell loss and dysfunction, leading to hyperglycemia. Islet amyloid, formed by aggregation of human islet amyloid polypeptide (hIAPP; amylin), contributes to progressive β -cell dysfunction/death in T2D. We previously showed that amyloid promotes islet interleukin-1 β (IL-1 β)

production, upregulation of Fas cell-death receptor, and activation of the Fas-mediated apoptotic pathway in β -cells. Importantly, islet α -cells were protected from amyloid toxicity via mechanisms yet to be identified. In this study, we examined the potential difference between Fas expression in α -cells and β -cells, before and after exposure to β -cell apoptotic factors, as a potential protective mechanism in α -cells.

Methods: Transformed α -TC1 and INS1 β -cells were cultured in normal or elevated glucose in the presence or absence of IL-1 β (1 ng/ml), fibrillogenic hIAPP (10 μ M) or non-fibrillogenic rat IAPP (rIAPP, 10 μ M; as control) for 12 hours (Fas) and 24 hours (TUNEL). Fas expression and apoptosis were detected by double immunolabelling for insulin/Fas (or glucagon/Fas) and insulin/TUNEL (or glucagon/TUNEL), respectively. The proportion of Fas and TUNEL-positive (apoptotic) α -TC1 and INS1 β -cells were quantified (n=3 independent studies).

Results: Fas was not detectable in untreated or rIAPP-treated INS-1 β -cells but it was markedly upregulated following treatment with hIAPP or IL-1 β , which was associated with elevated TUNEL-positive cells. Similarly, Fas was not detectable in untreated or rIAPP-treated α -TC1 cells and Fas upregulation occurred following hIAPP or IL-1 β treatment associated with increased TUNEL-positive cells, but to a much lesser extent than that observed in INS-1 β -cells.

Conclusion: These findings suggest that Fas upregulation mediated by amyloid or IL-1 β , two β -cell apoptotic factors associated with T2D, is significantly higher in β -cells than α -cells, resulting in much higher rate of apoptosis in β -cells. The lower Fas expression may be a protective mechanism in α -cells against apoptotic factors that cause β -cell apoptosis in T2D.

Quercetin Mediated CNS Targeting Investigation for Prevention and Management of Type II Diabetes Mellitus

Rashita Makkar¹, Tapan Behl²

¹Chitkara University, Department of Pharmacology, Rajpura, Punjab, India, ²University of Petroleum and Energy Studies, Department of Pharmacology, Dehradun, Uttarakhand, India

Purpose: Even though majority of blood glucose is utilized by brain, still a direct association between the brain and maintenance of glucose homeostasis remains unexplored to a huge extent. Type 2 diabetes mellitus is mainly characterized by the development of insulin resistance and the inability of glucose to enter different types of cells and neurons which results in cellular death due to starvation. The accumulation of excessive insulin in the blood during resistance towards it arises mainly due to incapability of the brain to utilize it for physiological functions and further leads to neuronal starvation and CNS complications.

Methods: The current study aimed to investigate the central origin of Type II diabetes mellitus and evaluate the effect of quercetin on cold-induced brain injury (CIBI) in Swiss albino mice. The mice were divided into four groups (n=6) and were subjected to cold brain injury, during which 30 mg/kg quercetin was orally administered in one of the groups. Glucose levels and behavioral parameters were investigated. The hippocampus of the mice was assessed at the end to evaluate oxidative stress and neuronal damage and degeneration.

Results: Results revealed that animals were highly anxious (elevated plus maze and open field), showed depressive like behavior (forced swim test), and displayed reduced locomotion (open field) in CIBI group. Quercetin alleviated behavioral dysfunction in CIBI group, significantly reduced anxiety, attenuated depression, improved cognitive dysfunction and normalized locomotor activity. Further, CIBI elevated the levels of oxidative stress markers (TBARS, nitric oxide), lowered antioxidants (catalase), altered expression of pro-inflammatory cytokines (IL-6, COX-2, IL-1 β , TNF- α) in the hippocampus and damaged hippocampal neurons.

Conclusion: Quercetin treatment significantly improved behavioral complications and lowered oxidative stress and prevented neural damage. In conclusion quercetin can efficiently prevent stress induced neurological complications by rescuing brain from oxidative and

inflammatory stress.

References

Rheumatol 2021 41(12): 2047-67

Identifying SHP2 allosteric inhibitors using In-silico screening, biophysical and molecular biological techniques

Maryam Jama, Marawan Ahmed, Anna Jutla, Carson Weithan, Jitendra Kumar, Tae Chul Moon, Frederick West, Michael Overduin, Khaled Barakat

University of Alberta

Purpose: The src homology region 2 (SH2) containing protein tyrosine phosphatase 2 (SHP2) is an oncoprotein and an emerging target for cancer treatment. Its overactivation is associated with tumour initiation, progression, and metastasis. Current research is focused on developing allosteric inhibitors targeting SHP2. Potent inhibitors such as SHP099 paved the road for this research. However, despite extensive efforts, SHP2 allosteric inhibitors have yet to reach the clinic. Identifying highly bioactive and selective SHP2 inhibitors will be necessary for drug development and to better understand SHP2 functions in malignancies. This study aimed to use computational modelling to identify novel SHP2 allosteric inhibitors and validate their activity through in vitro biochemical assays.

Method: Using *in silico* modelling, we screened over 6 million compounds against the allosteric site of SHP2. The compounds with the lowest free binding energy were selected for experimental testing using protein thermal shift assay (PTSA). Subsequently, the binding affinity of the compounds to SHP2 was confirmed using biolayer interferometry (BLI) assay. Lastly, the dose response of the three top compounds was investigated using DIFMUP as a substrate in a biochemical SHP2 inhibition assay.

Results: In silico modelling identified 26 top ranked hits with <-28kcal/mol. The PTSA validated three compounds (C8, B9, C2), which

exhibited a positive change in melting temperature. C8, B9, C2, and SHP099 were confirmed to bind to and inhibit SHP2's activity in the nanomolar range (See Table 1).

Conclusion: Our study demonstrates an effective screening methodology to identify active SHP2 allosteric inhibitors. The novel compounds demonstrated strong affinity and potent inhibition to SHP2, enabling further investigation of SHP2 in cancer.

Table 1. The dissociation constant and the inhibitory concentration of the compounds to SHP2

Compounds	KD (nM)	IC50 (nM)
C8	30	30±10
B9	70	40±5

References

1. Pádua, Ricardo AP, et al. "Mechanism of activating mutations and allosteric drug inhibition of the phosphatase SHP2." *Nature communications* 9.1 (2018): 4507.
2. LaMarche, Matthew J., et al. "Identification of TNO155, an Allosteric SHP2 Inhibitor for the Treatment of Cancer." *Journal of medicinal chemistry* 63.22 (2020): 13578-13594.
3. Song, Yihui, et al. "A multifunctional cross-validation high-throughput screening protocol enabling the discovery of new SHP2 inhibitors." *Acta Pharmaceutica Sinica B* 11.3 (2021): 750-762.

Evaluating the Impact of Amorphous Solid Dispersion Loading Level in Controlled Release Coated Beads by Experiments and Computer Simulation

Hao-Han (Ricky) Chang¹, Jamie Anne Lugtu-Pe¹, Xuning Zhang¹, Kuan Chen¹, Anil Kane², Xiao Yu Wu¹

¹University of Toronto, Toronto, ON, ²Patheon By Thermo Fisher Scientific, Mississauga, ON

Purpose

Multiparticulate dosage forms, such as controlled release amorphous solid dispersion (CRASD) membrane coated beads, are promising in preventing drug recrystallization and providing sustained drug release. However, optimal formulation design by experiments alone remains challenging. This work thus investigates how to tailor ASD loading level and quantity of beads for a given drug dose to achieve optimal release profile and drug utility using a poorly soluble drug, celecoxib. The release kinetics and extent of CRASD beads with varying loading levels were studied by experiments and computer simulations.

Method

Membrane-reservoir beads were prepared by coating an ASD layer containing celecoxib-polyvinylpyrrolidone onto MCC seeds, followed by an insoluble membrane layer using a fluid-bed coating system. Release profiles in pH 6.8 were obtained using various bead amounts at a fixed dose. A mathematical model for a bilayer bead was built with consideration of drug loading level, dissolution rate in the ASD layer, and diffusion through the membrane. The model was validated with experimental data and used to predict *in-vitro* profiles of various dosage design options using the Advanced Pharmaceuticals Computer Analysis and Design (AP-CAD) software.

Results

Among the CRASD beads with different ASD coating levels (3.5%, 5.4%, and 10% drug load), 5.4% drug load exhibited the optimal release profile, while 10% drug load resulted in slower release and reduced drug utility up to 18 hours. The release profile predictions by the AP-CAD software were in agreement with the experimental curves, suggesting that drug dissolution and total surface area of the beads are key factors of release kinetics impacted by the drug load level and number of beads.

Conclusion

The results of this work indicate that drug loading level in a CRASD bead formulation for a given dose can be tailored to achieve desired drug release profile and drug utility for oral administration.

References

J Pharm Sci 2016 105(9):2527-2544

J Control Release 2016 243:11-20

Investigating the effects of mild hyperthermia on immunogenic cell death induced by chemotherapy

Xuehan Wang¹, Pauric Bannigan¹, Christine Allen¹

¹University of Toronto, Toronto, ON

Purpose: Doxorubicin (DOX) is among the most widely used chemotherapy regimens and plays an important role in breast cancer treatment. Apart from cytotoxicity, DOX can induce immunogenic cell death where damage-associated molecular patterns (DAMPs) exposed by dying cells activate immune responses. To address the clinical concern of cardiotoxicity caused by free DOX and to overcome limited drug release associated with traditional liposomes, a thermosensitive liposomal (TSL) formulation of DOX (ThermoDox) has been developed and evaluated in clinical trials together with mild hyperthermia (HT). Our group has shown that the addition of immunotherapy to a TSL formulation of another chemotherapeutic agent in combination with HT results in an abscopal treatment effect, indicating a potential treatment strategy for metastatic spread. We are now investigating this effect for the potent ICD inducer DOX and expect it will result in a strong anti-tumor immune response. Here we evaluate the ICD effect of DOX +/- HT conditions *in vitro* as the first step.

Methods: The ICD effect at 37°C and 42°C was determined through DAMPs release in murine breast cancer 4T1 cells by flow cytometry, luminescence assay, and ELISA, respectively.

Results: Following DOX treatment calreticulin (CRT) exposure on the cell surface and high mobility group protein B1 (HMGB1) secretion were amplified, while increased release of ATP was noted. HT did not significantly enhance the overall DAMPs release.

Conclusion: HT did not effectively elicit an ICD effect *in vitro*, however it also did not compromise the ICD effect induced by DOX. Increased incubation temperature may not be fully representative of the effects of HT *in vivo*. Further investigation of immune response of ThermoDox and HT treatment in an animal model would illustrate if this approach can modulate the immune system more accurately.

Novel Piperine Derivatives as Beta Amyloid Aggregation Inhibitors

Shirley Wang

University of Waterloo

Purpose: Alzheimer's Disease (AD) is a neurodegenerative disease largely associated with the brain's accumulation of amyloid-beta ($A\beta$) aggregates.¹ Recently, a naturally derived product known as piperine was discovered to have excellent anti-amyloid properties but possesses poor pharmacokinetic properties.² This makes it an attractive structural template for developing potentially novel AD therapies.

Method: Currently, the mechanism of action regarding piperine's anti-aggregation properties is poorly understood. Therefore, this project aims to investigate the $A\beta$ 42-binding interactions of piperine and its derivatives by i) synthesizing a scaffold of piperine derivatives using organic and analytical chemistry techniques (1H and ^{13}C NMR, flash chromatography, LC-MS and HR-MS), ii) conducting fluorescence assays and transmission electron microscopy (TEM) experiments to discover the $A\beta$ 42-aggregation kinetics and morphology respectively in the presence of piperine derivatives, iii) assessing compound cytotoxicity towards HT22 mouse hippocampal neuronal cells, and v) performing computational modeling studies to understand the chemical features required to bind and inhibit $A\beta$ 42.

Results: The optimized synthetic protocols led to the successful synthesis and characterization of novel piperine derivatives. *In vitro* screening by aggregation kinetics and TEM studies led to identifying one derivative (**4c**) that exhibited superior inhibition of $A\beta$ 42 compared to

piperine itself (38% at 25 μ M). Additionally, in silico studies docking the top compounds into the seeding region of the A β 42 pentamer model correlated well with the in vitro assays. Lastly, the cytotoxicity assays using HT22 cells showed >90% cell viability when tested up to 25 μ M for each derivative.

Conclusion: This is the first report to identify novel piperine derivatives that are demonstrated to directly bind A β 42 and reduce its aggregation potential, exhibiting superior anti-aggregation properties compared to its parent compound piperine. Overall, these results show great promise for further development of novel anti-amyloid agents that can potentially be used to combat AD.

References

- (1) Eur. J. Med. Chem. 2016, 113: 258-272.
- (2) Beni-Suef Univ. J. Basic Appl. Sci. 2022, 11: 1-24.

Classifying comb polymer monolayers by structure and sieving properties using simulations and machine learning

Nicole Drossis¹, Marc Gauthier², Hendrick de Haan¹

¹Ontario tech university, ²INRS

Purpose Protein-polymer bioconjugates can have a wide variety of applications, and given the many possible combinations of proteins and polymer structures, there is a very large parameter space to be explored that is difficult to fully scope experimentally. This work focuses on simulating comb polymer monolayers with different dimensions and densities on surfaces of different curvature to observe how their structure changes, and develop a tool using machine learning that will give a user information about the structure and permeability of a comb polymer monolayer when provided with the polymer's dimensions, grafting density and surface curvature.

Methods Coarse grained simulations were performed scoping the parameter space. From these simulations a large dataset was created,

containing measured values of polymer conformation such as polymer density profiles, radius of gyration, etc., as well as monolayer permeability cutoff measured by observing collisions between substrate particles and the surface, and seeing how large the substrate can get before no collisions are observed. For the machine learning tool, a feed-forward neural network was trained on this dataset.

Results It was found that there is a strong inverse correlation between permeability cutoff and the average density of polymer beads in the volume around the surface. Additional effects were observed such as curvature resulting in a decrease in density, due to there being more space available farther away from the surface when it is curved, and the confinement of polymers on flat surfaces at high density resulting in them being more extended.

Conclusions This work scopes a wide range of parameters, observing and classifying the structure of comb polymer monolayers and how it relates to their permeability. A machine learning tool was created to help with future work, to allow a user to pick their polymer parameters by inputting their desired outcome for structure or permeability.

Transcriptional regulation of cytochrome P450 1a2 by arsenic trioxide (ATO) in murine hepatoma Hepa-1c1c7 cells

Mahmoud A. El-Ghiaty, Mohammed A. Alqahtani, Ayman O.S. El-Kadi
University of Alberta, Edmonton, AB

Purpose: Arsenic is an occupational and environmental contaminant that imposes threat to humans. Arsenic trioxide (ATO) is an arsenical that has been exploited for treating acute promyelocytic leukemia (APL), with a strong potential for treating other tumors. However, ATO efficacy is associated with serious toxicities whose mechanism is yet to be resolved. Several studies have reported the ability of different arsenicals to modulate cytochrome P450 1a2 (Cyp1a2) enzyme, whose activity is crucial for activating/detoxifying drugs/procarcinogens. Therefore, this study aimed to investigate the effects of ATO on Cyp1a2 in absence and presence of its inducer, 2,3,7,8-tetrachlorodibenzo-p-dioxin (TCDD),

using in-vitro model.

Methods: Mouse hepatoma Hepa-1c1c7 cells were treated with ATO (0.63, 1.25, and 2.5 μ M) in the absence or presence of 1 nM TCDD for 6 and 24 h. Cyp1a2 expression was assessed at mRNA and protein levels using qPCR and Western blotting, respectively. Cyp1a2 activity was measured by 7-methoxyresorufin O-demethylase (MROD) assay. Luciferase reporter gene assay utilized xenobiotic response element (XRE)-transfected Hepa-1c1c7 cells.

Results: ATO significantly increased TCDD-mediated induction of Cyp1a2 mRNA, protein, and catalytic activity, while basal Cyp1a2 was increased only at mRNA and protein levels. Mechanistically, 2.5 μ M ATO significantly increased basal and inducible aryl hydrocarbon receptor (AHR)-dependent luciferase reporter signal. At the same concentration, ATO significantly increased AHR level in the nuclear protein fraction.

Conclusion: We demonstrated that ATO up-regulates Cyp1a2 transcripts, protein, and catalytic activity in Hepa-1c1c7 cells, at least partly, through a transcriptional mechanism mediated by enhancing AHR nuclear recruitment and subsequent activation of its regulatory element. This implies the possible involvement of ATO in clearance-related pharmacokinetic or toxicokinetic interactions with the substrates of Cyp1a2.

This work was supported by the Natural Sciences and Engineering Research Council of Canada (NSERC) Discovery Grant [RGPIN 250139] to A.O.S.E. M.A.E is recipient of the Rachel Mandel Scholarship.

References

1. EXCLI J. 2021 Jul 12;20:1184-1242.
2. Chem Biol Interact. 2022 Sep 1;364:110049.

Designing Nanomedicines for Breast Cancer Therapy

Saba Abbasi Dezfouli, Amarnath Rajendran, Remant K.C., Hasan Uludag

University of Alberta, Edmonton, Alberta

Background. In 2020, breast cancer became the most commonly diagnosed cancer worldwide ^[1]. Conventional chemotherapies have major side effects mainly due to their inability to specifically target cancerous cells. Alternatively, gene therapy which make use of both viral and non-viral carriers piqued the interest about 40 years ago. Nonviral carriers are preferred since they display lower immunogenicity and production costs. Short interfering RNAs (siRNA) carrying nanoparticles have high potentials to overcome the non-specificity of conventional therapies and reduce the expression of disease-associated proteins by mimicking the naturally occurring RNA interference mechanism. Lipid-substituted polyethyleneimine (PEI) polymers (lipopolymers) have been demonstrated to be efficient non-viral carriers in many cancer models since they provide the perfect balance for cell penetration and nanoparticle packaging ^[2].

Methods. To improve therapies, our goal is to engineer novel non-viral lipopolymer carriers specifically for the treatment of breast cancers and to optimize our nanocomplexes by experimenting with a variety of additives to nanoparticles to obtain high gene silencing through siRNA activity with the least amount of nonspecific toxicity.

Results. We first optimized our polyplexes in GFP+ MDA-MB-231 cells to effectively silence the GFP gene using the GFP siRNA. Inclusion of phosphate pH 8.0 as complex preparation media and N-Lauroylsarcosine Sodium Salt as additive to enhance dissociation of siRNA, achieved ~80% silencing with the least amount of undesired cytotoxicity. Furthermore, these effects were shown to be persistent for at least 6 days. *Survivin* gene was then selected to test our complexes for endogenous gene silencing in MDA-MB-231 cells since there is no strong drug (i.e., small organic molecule) for inhibition of its oncogenic activity. qRT-PCR analysis and MTT assay revealed >80% silencing and ~70% cell death by the same formulation.

Conclusion. The results show improved formulations for development of modified PEI-lipopolymers to target selected endogenous genes in MDA-

MB-231 cells.

References

1. WHO World Cancer Day 2021: Spotlight on IARC Research Related to Breast Cancer. (2021). Available online at: <https://www.iarc.who.int/featured-news/world-cancer-day-2021/> (accessed May 02, 2021).
2. Meneksedag-Erol, D., Kc, R.B., Tang, T. and Uludag, H., 2015. A delicate balance when substituting a small hydrophobe onto low molecular weight polyethylenimine to improve its nucleic acid delivery efficiency. *ACS Applied Materials & Interfaces*, 7(44), pp.24822-24832.

Use of Paramagnetic Spin Probes to Investigate Fluidity of Polymeric Micelles

Lusine Tonoyan¹, Munira Sirazum², Afsaneh Lavasanifar², Arno Siraki²

¹Applied Pharmaceutical Innovation, Faculty of Pharmacy & Pharmaceutical Sciences, College of Health Sciences, University of Alberta, ²Faculty of Pharmacy & Pharmaceutical Sciences, College of Health Sciences, University of Alberta

Background. Electron paramagnetic resonance (EPR) spectroscopy is the gold standard for studying free radicals. Spin probes, which are stable free radicals, can be used to study the dynamics of viscosity and fluidity in a particular environment, such as in polymeric micelles used for drug delivery. EPR spectroscopy spin probes can provide a range of parameters, such as spectroscopic rotational time (τ), which can be used to determine the fluidity of a polymeric micelle membrane. Higher τ values reflect a less fluid, more rigid membrane. Other parameters that can be calculated using EPR spectroscopy include the spectroscopic partition parameter, F , which reflects the distribution of spin probes between the membrane and the surrounding environment.

Methods. To evaluate the fluidity of polymeric micelles, we mixed empty and drug-loaded polymeric micelles (PEO-PBCL and PEO-PCL) with two stable nitroxyl radical probes, methyl 5-doxyloleate and 16-doxyloleic acid, and kept them in the dark for different time periods at varying temperatures. SDS and H₂O were used as controls. EPR spectra

were then obtained and analyzed using a Bruker E500 spectrometer.

Results. This study showed that the values of τ and F could be calculated from the EPR spectra of different micelle preparations. The 16-doxylstearic acid probe produced more intense spectra than the methyl 5-doxylstearate probe, but the τ and F values correlated for both probes. Higher temperatures were found to increase the fluidity of the micelles, and there were differences in the probe interaction between different micelle preparations and drug-loaded micelles.

Conclusions. Overall, this methodology provides a useful approach to studying micelle membrane fluidity, and the findings of this study may have implications for drug delivery and therapeutic activity. By providing a deeper understanding of the fluidity of micelle membranes, these techniques may help to optimize drug delivery systems that are more effective and efficient.

Extracellular Matrix Binding Vehicles for Local Delivery of Therapeutic Proteins

Ava Ettehadolhagh

Department of Chemistry and Chemical Biology, McMaster University,
Hamilton, Ontario, Canada

Purpose: The therapy suppressive tumour microenvironment (TME) continues to hinder anti-cancer therapies. Local delivery of therapeutic proteins, including systemically toxic factors, is of increasing need for the enhancement of immunotherapeutic bioactivities.¹ To this end, we are developing vehicles that immobilize within the extracellular matrix (ECM) and sustain protein release. These vehicles have the potential to be used for different types of solid tumours. In this study, they would be used for delivering the cytokines such as interleukin 15 (IL-15) and interferon-gamma (IFN- γ) into the glioblastoma TME.²

Method: A low-fouling copolymer, poly(carboxybetaine-co-N-(3-aminopropyl)methacrylamide hydrochloride) (pCB-APMA), was

synthesized through RAFT polymerization. IL-15 and IFN- γ were expressed, purified and their biological activity was examined using cell assays. Click chemistry was used to graft the proteins and collagen-binding peptides to the pCB copolymer. The binding affinity between carriers and collagen type 1 was demonstrated by tracking immobilization and diffusion of fluorescently labelled carriers within collagen hydrogel. In vitro models were established to examine the bioactivity of the carriers in the presence of T-cells and macrophages

Results: pCB-APMA copolymer synthesis was first confirmed by NMR and gel permeation chromatography (GPC) to yield a copolymer of 31 kDa with a dispersity of 1.2. A T-cell proliferation assay was conducted to ensure the bioactivity of IL-15, with an effective concentration of 0.1 nM. Production of the carrier, pCB-APMA copolymer with graft IL-15 (fluorescently labelled) and collagen binding peptides, was confirmed by SEC and fluorescent measurements. Binding to collagen was confirmed by fluorescent micrographs, surface plasmon resonance studies are ongoing. Biological activity within multicellular models in collagen hydrogels is under investigation.

Conclusion: ECM binding vehicles for local sustained protein release will aid in the local delivery of therapeutic proteins to alter TME and promote immunotherapies. Screens will be conducted in multicellular spheroid models to identify bioactive formulations.

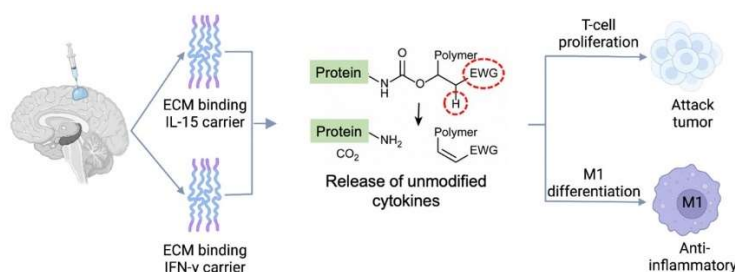


Figure 1. ECM binding vehicles for local and sustained protein release. The linker between the therapeutic protein and pCB-APMA will contain hydrolytic carbamate bonds with highly tunable half-lives from hours, days to weeks for tunable protein release.

References

1. Front. Med. Technol 2021 3: 67
2. Proc. Natl. Acad. Sci. U. S. A. 2013 110: 8158-8163.

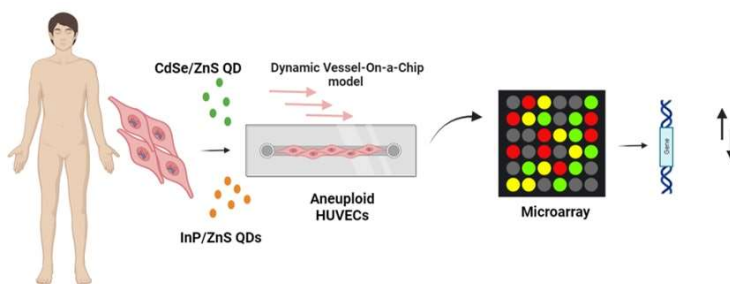
Transcriptomics to evaluate the impact of quantum dots on aneuploid endothelial cells in a dynamic vessel-on-a-chip model

Yasmin Abdelkader¹, Madhumita Suresh¹, Tulio Lopera¹, Simranpreet Dhaliwal¹, Shahla Shojaei¹, Qian Liu¹, Pingzhao Hu¹, Seiichiro Ishihara², Max Anikovskiy¹, Hagar Labouta¹

¹University of Manitoba, Winnipeg, MB, ²University of Calgary, Alberta, AB

Aneuploidy is a characteristic feature of the dysfunctional endothelial cells lining the angiogenic blood vessels surrounding solid tumors. [1] Nanoparticles (NPs) have been used as an effective drug carriers for tumor targeting and in other diseases. However, little is known about aneuploid endothelial cell responses to nanoparticles under conditions mimicking tumor angiogenic blood vessels. To this end, we developed a dynamic vessel on-a-chip model using human umbilical vein endothelial cells (HUVECs) and induced aneuploidy using monastrol. Two different types of quantum dots (QDs) were applied, CdSe/ZnS and InP/ZnS QDs, on aneuploid models versus euploid controls. Dynamic experiments were conducted under a shear stress 1 dyne/cm² and a flow rate of 65µl/min [2] and were compared to static experiments. At the end of the experiments, RNA was extracted and analyzed using microarray to detect the genetic changes in aneuploid HUVECs versus euploid HUVECs in dynamic and static conditions. Transcriptomic results revealed a significant impact of aneuploidy together with dynamic conditions, evident as a down-regulation of cell cycle checkpoints and cell division. Dynamic aneuploid HUVECs treated with CdSe/ZnS or InP/ZnS showed an apoptotic and inflammatory response via upregulation of PMAIP1 gene for apoptosis and Smad6, HSPA1A, and HSPA1B genes for inflammation. Nevertheless, dynamic conditions favor the expression of important genes related to shear stress KLF4 and tight junction OCLN. Network analysis was created with Cytoscape that showed the molecular interaction networks in gene expression profiles. We present a novel approach using vessel-on-a-chip and transcriptomics to identify molecular responses of different endothelial cell models, in which dynamic aneuploidy showed the greatest alterations in genes and

biological pathways compared to other models.



References

- [1] Dev Cell. 2021;56 :2427-2439
- [2] TrAC.2019; 117:186-199

Formulation and evaluation of starch-based spray dried microcapsules loaded with essential oils for oral administration

Georgia De Flavis, Anyston Chin, Jorja Giannopoulos, Sydney Lengacher, Mohamed Nabil Khalid

Biopharmaceutical Production Technology Department, John Abbott College, 21275 Lakeshore Road, Sainte-Anne-de-Bellevue, Quebec, Canada, H9X 3L9

Purpose: To prepare and evaluate starch-based spray-dried microcapsules loaded with essential oils (EO). EO are used for flavoring in foods, cosmetics, and personal hygiene products. They are affected by external factors such as light, oxygen, and temperature. To reduce these effects, microencapsulation using spray-drying was considered.

Method: Starch 7.5% (w/w) was first dispersed in a phosphate buffer pH 6.8 using a low shear mixer. Solutions of Xanthan gum at 1 and 1.5%, and Cekol 150 at 1 and 2 % w/w were prepared in deionized water using a high shear mixer. Kollidon VA-64 at 5% w/w was added as viscosity reducer. Mixtures were then prepared using a low shear mixer. Orange and peppermint oils were added with loading concentrations of 20 and 30% w/w each. Mixtures were spray-dried using a lab scale spray-dryer with 1.25 L batch size. The resulting microcapsules were collected, potential interactions or degradation were evaluated using FTIR, and SEM was used to evaluate size and morphology.

Results: Spray-drying process was successfully performed, and critical process parameters optimized. FTIR spectroscopy analysis of the spray-dried microcapsules showed the absence of chemical interactions between EO and other ingredients in the formulation. SEM observation of the spray-dried powder showed spherical smooth microcapsules with size ranging from 1 to 20 μm . The sphericity of microcapsules was better when using Xanthan gum at 1.5% w/w.

Conclusion: Stable starch-based microcapsules loaded with different food grade EO were successfully prepared using spray-drying technique at lab scale. These microcapsules represent a promising device insuring the stability of EO.

References

1. US patent, Khalid et al. 2014/0206704
2. Int J Res in Pharma Sci 2019 10-4: 3616-3625

Pharmacokinetics of pimozone in Sprague-Dawley rats and application of Bayesian forecasting to understanding the impact of obesity

Hamdah Al Nebaihi, Seyed Amirhossein Tabatabaei Dakhili, John

Ussher¹, Dion Brocks

University of Alberta, Edmonton, AB

Purpose: To understand the impact of obesity on the pharmacokinetic parameter (PKP) of the antipsychotic drug, pimozone.

Methods: To gain estimates of the mean and SD of pimozone in Sprague-Dawley rats, five male jugular-vein cannulated rats were administered 10 mg/kg pimozone (PMZ) as oral gavage. Blood samples were collected for 24 h to determine the full concentration vs. time curve (rich sampling) and PKP. Other groups of male and female rats (n=5) were given standard (Control) or high-fat diet (HFD) for 9 wk. They were given 10 mg/kg PMZ po, and 2 blood samples were collected per rat via the saphenous vein. PMZ blood concentrations were measured using LC-MS/MS. Bayesian and compartmental analysis was done using PKSolver and PKB-est, respectively.

Results: PMZ followed a one-compartment model with CL/F, Vd/F and t_{max} of 17±6.7 L/h/kg, 67±18 L/kg, and 4.0±1.3 h, respectively in the cannulated male rats. Bayesian forecasting was validated using randomly selected concentrations from these rats; CL/F was well correlated between rich and sparse sampling estimates. The Bayesian estimates from sparse sampling in the dietary phase were 21±13, 4.7±2.3, 17.5±8.8 and 6.9±2.5 L/h/kg for CL/F and 57±9.1, 27±10.7, 73.4±5.3 and 38±6.6 L/kg for Vd/F, in the male Control, male HFD, female Control and female HFD groups, respectively. The CL/F and Vd/F were reduced by HFD in male rats, and Vd/F in female rats, compared to their respective Controls (p<0.05). A trend toward decreased CL/F was observed in female HFD (p=0.051). No significant differences were apparent between the PKP of cannulated younger male rats and Control

female or male rats.

Conclusion: Obesity, which can decrease CYP3A expression ⁽¹⁾, was associated with a decrease in the CL/F of the CYP3A substrate, PMZ. Bayesian forecasting provided promise in a preclinical study to estimate PKP, where only sparse blood concentrations were available (dietary arm).

(1) J Pharm Sci 2020 109: 1204-1205

Effect of Toll-like Receptor (TLR)-7 Mediated Maternal Immune Activation on Placental Proteome and Expression of Transporters.

Mario Riera Romo, Eliza McColl, Micheline Piquette Miller

Department of Pharmaceutical Sciences, Leslie Dan Faculty of Pharmacy, University of Toronto

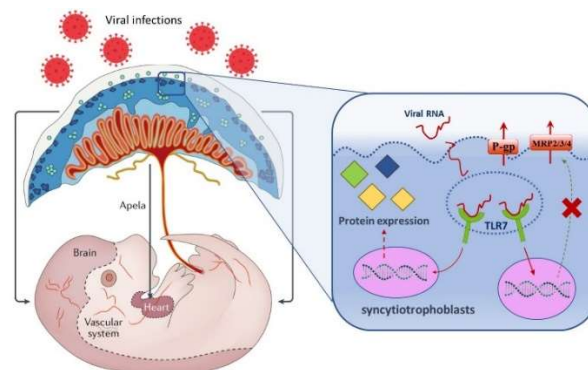
Purpose: Infections during pregnancy can adversely impact fetal development by aberrantly activating the maternal immune system¹. Single-stranded RNA viruses such as influenza and SARS-CoV-2 stimulate immune responses through activation of TLR-7; thereby impacting production of numerous proteins². Our lab has previously found that maternal disease alters the expression of placental transporters in humans and animal models. Therefore, using a pregnant rat model, our goal was to examine the impact of TLR7 activation and associated inflammation on drug transporter expression and the placental proteome.

Methods: Pregnant SD rats were administered a single dose (5 mg/kg, i.p.) of the selective TLR-7 agonist, imiquimod (IMQ) on gestational day 14. Expression of transporters and cytokines were measured at 6hr (n=4/group) and 48hr (n=8/group) post-injection via qRT-PCR and protein expression of P-glycoprotein was measured by immunodetection. The placental proteome was examined at 48 hr using LC/MS/MS.

Results: Transcript levels of interferon regulatory factor (IRF)-7, were increased by 20 and 200 fold in the placenta and liver of IMQ treated dams, respectively, indicating TLR-7 activation. IMQ treatment

dramatically increased placental and hepatic transcript levels of IL-6 as well as hepatic levels of TNF- α . The mRNA expression of several drug transporters (Oatp1a2, Oct3, Octn2, Ent1, Mdr1b, Mrp4) and protein expression of P-glycoprotein were significantly decreased in IMQ placenta. Proteomic analysis demonstrated IMQ activation of numerous pathways in placenta including oxidative stress, immune activation, vesicular secretion and proteolytical activity.

Conclusions: TLR7 activation in pregnancy stimulated the maternal and fetal immune system resulting in dysregulation of the placental proteome, particularly pathways involved in oxidative stress and immune responses. Moreover, this resulted in decreased placental expression of P-glycoprotein which could increase fetal exposure to potential harmful substrates. Overall, these changes could have potentially adverse effects on maternal and fetal health indicating a need for further investigation.



References

Clin Transl Sci 2020 13: 580-588

The Impact of Preeclampsia-associated Downregulation of Bcrp on Maternal and Fetal Drug Disposition of Rosuvastatin in Rats

Wanying Dai, Micheline Piquette-Miller

University of Toronto, Toronto, ON

Purpose: Recent studies in our laboratory have demonstrated downregulation of breast cancer resistance protein (Bcrp/Abcg2) in

placenta obtained from women with preeclampsia (PE). Pregnant women with PE are generally prescribed medications to manage disease progression and many of these drugs are substrates for Bcrp. Bcrp is highly expressed in placenta and plays an important role in preventing xenobiotics from crossing the placenta and entering the fetal compartment. However, there are limited studies on the impact of PE and Bcrp downregulation on fetal drug exposure. Use of preclinical models is an important approach. Thus, we characterized the impact of PE on Bcrp expression in a rat model of PE and used this model to examine maternal and fetal biodistribution of the Bcrp substrate rosuvastatin (RSV).

Methods: PE was induced by daily administration of low-dose endotoxin (0.01-0.04mg/kg) to rats on gestational days (GD)13 to 16. Urine was collected. PE and control rats received RSV (3mg/kg IV) on GD18, and were sacrificed at 0.25, 2.5 and 4hr. RSV levels were measured by LC-MS/MS, plasma cytokines by ELISA and placental expression of Bcrp by qRT-PCR and immunodetection.

Results: PE rats shared similar symptoms with PE patients, including proteinuria, and increased pro-inflammatory cytokines, TNF- α and IL-6. Transcript and protein expression of Bcrp were significantly decreased in the placentas of PE rats on GD18. The downregulation of BCRP was associated with higher 4hr ratio of fetal tissue:maternal plasma concentrations of RSV in the PE group, indicating increased fetal drug accumulation. RSV plasma protein binding was not significantly affected.

Conclusion: Overall, our results demonstrated that the downregulation of placental BCRP in PE is associated with increased fetal accumulation of its substrates. Furthermore, the PE rat model may be useful to further examine the impact of PE on maternal and fetal drug disposition for other drug substrates.

References

Clin Transl Sci 2020 13: 580-588

Can in vitro data predict in vivo performance of dermatological products?

Seeprarani Rath, Isadore Kanfer

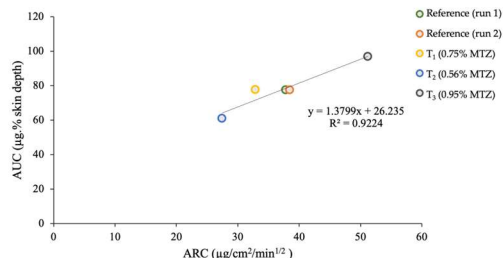
Leslie Dan Faculty of Pharmacy, University of Toronto

Purpose. Bioequivalence (BE) of products intended to be absorbed into the systemic circulation involves a comparison of drug concentrations of the test and reference products following administration to healthy human subjects. However, for topical dermatological products intended for local action, clinical trials in patients are generally required since these products are not intended to be absorbed into the systemic circulation. More recently, in vitro release testing (IVRT) has been accepted for use as a biowaiver for some such products. A dermatopharmacokinetic approach involving tape stripping (TS) has been demonstrated as an effective surrogate method to demonstrate topical BE.

Method. We describe the use of IVRT to predict in vivo performance of creams containing metronidazole (MTZ) by correlating the IVRT data¹ with TS data² from human subjects. While IVRT is used to characterize the release of drug from topical semisolid dosage forms across a synthetic membrane into a suitable receptor medium, TS involves sequential removal of unimolecular layers of the stratum corneum (SC) with an adhesive tape and helps to determine the drug amount in SC. The IVRT parameter, apparent release constant (ARC) was correlated with the TS parameter, area under the curve (AUC). A graph of AUC vs ARC was plotted in an attempt to establish a level C correlation (Figure 1). The BE limits were computed for these parameters based on the regulatory acceptance criteria.

Results. The results showed that in order to predict BE using IVRT studies, the values of ARC need to be between 30.50 and 47.67 when comparing test and reference creams containing MTZ.

Conclusion. IVRT has the potential to predict in vivo performance of topical MTZ creams and, with further investigation and refinement, it may be used to justify a biowaiver for topical products to make them more accessible and affordable to the wider population.



References

1. *Pharmaceutics* 2020, 12(2), 119
2. *J. Pharm. Pharm. Sci.* 2020, 23, 437-450

In vitro release testing (IVRT) to evaluate Q1/Q2/Q3 attributes of marketed topical clotrimazole creams

Hannah Wellington¹, Seeprarani Rath², Isadore Kanfer²

¹Faculty of Pharmacy, Rhodes University, South Africa, ²Leslie Dan Faculty of Pharmacy, University of Toronto

Purpose. To demonstrate the utility of IVRT in evaluating the qualitative (Q1), quantitative (Q2) properties and arrangement of matter (Q3) of topical clotrimazole (CLZ) creams from two countries - South Africa (SA) and Canada. All products were creams containing 1% CLZ intended for topical application. Hence, a validated IVRT was used to assess “sameness” and/ or detect differences, if any, between globally marketed CLZ creams.

Methods. A Hanson vertical diffusion cell (VDC) system equipped with six VDCs was used to characterise the release of CLZ through a polyethersulfone (PES) membrane into a receptor fluid consisting of phosphate buffer pH 7.4: ethanol 50:50%v/v, which was continuously stirred at 600 rpm over a period of six hours. Comparative IVRT was performed in accordance with the FDA’s SUPAC-SS guidance¹. Five SA-marketed generics were compared with the SA reference product, followed by a comparison between reference products from SA (R₁) and Canada (R₂) as well as a Canadian-marketed generic product (T₁), and two additional compounded test creams involving different excipients and manufacturing procedures (T₂ and T₃).

Results. All five SA-marketed generic creams showed pharmaceutical inequivalence to the SA reference product (Figure 1) indicating

Q1/Q2/Q3 differences between the products. Creams R_1 , R_2 and T_3 , containing the same excipients (Q1/Q2) had significantly higher release rates compared to T_1 and T_2 (Figure 2). The release rate of T_2 was the slowest possibly due to the presence of paraffin and propylene glycol. This illustrates that Q1/Q2 differences can significantly impact the drug release rates. Interestingly, despite containing the same excipients as both reference products, cream T_1 had a substantially lower release rate which could be attributed to Q2/Q3 differences.

Conclusion. The IVRT method displayed the requisite ability to discriminate between several marketed 1% CLZ creams, some with relatively insignificant differences and others with substantially dissimilar attributes relating to Q1/Q2/Q3.

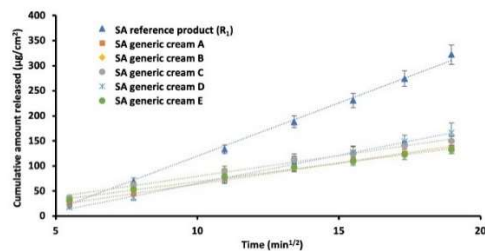


Figure 1. Comparative IVRT profile of SA reference and generic creams containing 1% CLZ

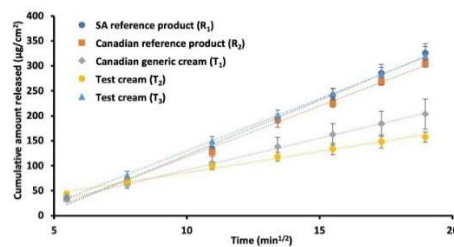


Figure 2. Comparative IVRT profile of 1% CLZ reference creams from SA and Canada (R_1 and R_2), Canadian generic (T_1) and test creams (T_2 and T_3)

References

1. US Food and Drug Administration. Guidance for Industry: Nonsterile Semisolid Dosage Forms, Scale-up and Post Approval Changes, Chemistry, Manufacturing, and Control; In vitro Release Testing and In vivo Bioequivalence Documentation (SUPAC-SS); Center for Drug Evaluation and Research: Rockville, MD, USA, 1997.

In Situ-Gelling and Hydrophobic Starch Nanoparticle (SNP)-based Nanoparticle Network Hydrogels (NNH) for the Intranasal Delivery of Olanzapine as a Safe and Effective Schizophrenia Treatment

Andrew Lofts¹, Matt Campea¹, Erica Winterhelt¹, Ram Mishra¹, Todd Hoare¹

¹McMaster University

Introduction: It is estimated that 1 in 300 of the global population suffers from schizophrenia. Intranasal (IN) delivery offers potential to deliver olanzapine, an atypical antipsychotic, directly to the brain, reducing the problematic systemic absorption of established oral treatments [1].

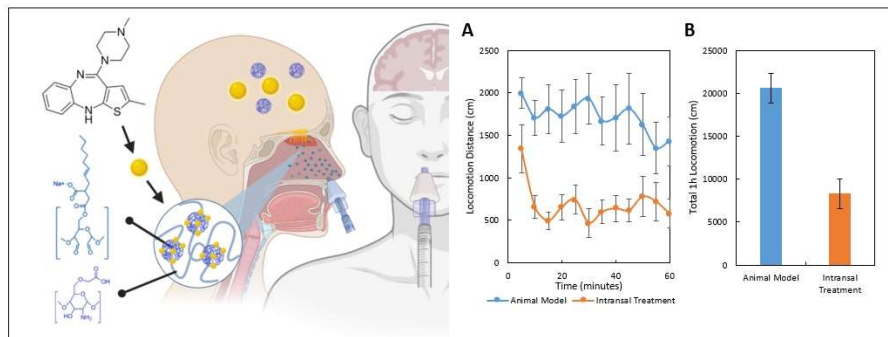
We have designed a sprayable starch nanoparticle (SNP) network hydrogel (NNH) that gels *in situ* within the nasal cavity when co-extruded with mucoadhesive carboxymethyl chitosan (CMCh) [2]. Functionalization of the SNPs with hydrophobic chains creates hydrophobic domains within the hydrogel for drug loading and complexing, enabling controlled release of olanzapine-loaded SNPs from the NNH depot into the nose-to-brain pathway (Fig1).

Methods: SNPs were first functionalized with hydrophobic groups via octenyl succinic anhydride followed by oxidation via sodium periodate to introduce aldehydes. The degree of functionalization was assessed via titration, size via dynamic light scattering, and hydrogel degradation via gravimetric analysis. Amphiphilic behaviour was tested via hanging drop and solvent creaming. SNP cytocompatibility was tested in human brain (SH SY5Y) and nasal cell (HNEpC) lines via MTT assays. Formulation efficacy is tested via an induced rat schizophrenia-mania model (amphetamine locomotion and ambulation) and IN delivered hydrogels and drugs.

Results: SNPs were successfully functionalized with OSA and CHO groups (0.1-0.2DS, 0.25DS). The SNPs were ultrasmall in size (10-25 nm), miscible in several solvents and low surface indicative of amphiphilic behavior. Resulting NNHs form within minutes and degrade over several hours enabling slow drug release. All SNPs were cytocompatible (>70% viability) and could penetrate cells. Animal models demonstrated that IN is an effective therapy with the hydrogel successfully controlling drug release (Fig1. A-B).

Conclusions/Impact: *In situ*-gelling CMCh/SNP NNH provide a biodegradable and safe method of IN olanzapine delivery directly to the brain bypassing systemic toxicity, using customized SNPs that exhibit high epithelial penetration and drug complexing properties to maximize

delivery.



References

CNS Drugs. 2022; 36(7): 739-770

J Control Release 2021 330:738-752

The quantifications of multiple tyrosine- and tryptophan-derived protein bound uremic toxins using liquid-chromatography tandem mass-spectrometry

Ala'a Al Dajani, Yan Rong, Tony Kiang
 University of Alberta, Edmonton, AB

Purpose: Indoxyl sulfate (IS), indoxyl glucuronide (IG), *p*-cresyl sulfate (*p*CS), and *p*-cresyl glucuronide (*p*CG) are uremic toxins derived from amino acids in the gut. The accumulations of these compounds under poor renal function have been associated with cardiorenal complications. This study developed a sensitive and high-throughput ultra-high performance liquid chromatography-tandem mass spectrometry (UPLC-MS/MS) assay to simultaneously measure these compounds.

Methods: Instrumentation consisted of the Shimadzu LC-MS-8050 (Kyoto-Japan) fitted with the Raptor-biphenyl column (100 x 2.1mm-2.7 μ m; Restek-USA). The best ionization mode (electrospray, atmospheric, dual-approach; under positive or negative ionization) was determined, followed by parent-daughter spectra scanning for either single ion (SIM) or multiple-reaction monitoring (MRM). All ionization parameters (below) were optimized. Deuterated analytes (i.e., IS-d4,

*p*CS-d7, and *p*CG-d7) served as internal standards.

Results: Negative electrospray-ionization yielded the highest sensitivity with the following MRM transitions (m/z) for IS (212.20> 76.90), *p*CS (187.20> 79.85, 107.00), *p*CG (283.25> 107.05, 112.95), IS-d4 (215.9> 136.05), *p*CS-d7 (194.20> 114.10, 79.90), and *p*CG-d7 (290.00> 113.00, 114.05). IG was best detected in SIM (m/z 309.27). The optimal drying, heating, and nebulizing gas flow (10, 10, and 1.5 L/min); interface and conversion-dynode voltages (4.5V and 10kV); interface, desolvation-line, and heat-block temperatures (300 °C, 200°C, and 400°C); collision-induced dissociation-gas (270kPa), and additives (10mM ammonium acetate and 0.1% v/v formic acid) for ionization were determined. The ideal methanol gradient consisted of 5% (0.0-1.0min), 95% (1.5-5.0min), and 5% (7.0-12.0min) with a total run-time of 12min. The retention times were IS (3.04min), IG (3.08min), PCS (3.11min), PCG (3.14min), IS-d4(3.03min), PCS-d7(3.11min), and PCG-d7 (3.14min). A lower limit of quantitation of 0.45ng/mL makes this assay more sensitive compared to the literature.

Conclusion: We have developed a sensitive and high-throughput LC-MS/MS assay for the simultaneous quantification of IS, IG, *p*CS, and *p*CG. After validation, this assay will be used to investigate the toxicokinetics of these compounds.

Development of Lipid-Based Drug Carriers for Oral Delivery of Cannabidiol

Behnoush Kermanshahi¹, Gokce Alp¹, Andrea Olaizola², Brendan Morris-Reade¹, XuXin Sun³, Tom Skrinikas⁴, Jessica Kalra^{1, 5}

¹Langara Applied Research Center, ²University of British Columbia,

³Experimental Therapeutics, BC Cancer Agency, ⁴Nanovation

Therapeutics, ⁵UBC Faculty of Pharmaceutical Sciences

Purpose: Cannabidiol (CBD) is considered to be the most favorable phytocannabinoid with potential pharmaceutical properties [1]. However, one challenge in pursuing CBD as a therapeutic agent lies in its poor water solubility which limits its bioavailability. To improve the

biodistribution of CBD, encapsulation within nanoparticles is of great interest. Lipid-based drug nanocarriers possess several advantages including biocompatibility, ability to solubilize hydrophobic drugs, and high encapsulation efficiency [2]. To evaluate lipid-based nanoparticles as delivery systems for CBD, three different lipid-based formulations were designed: 1. nanostructured lipid carriers (NLC) consisting of fatty acids and surfactants, 2. liposomes consisting of phospholipids and cholesterol, and 3. self-emulsifying drug delivery systems (SEDDS) consisting of oil, surfactant and cosurfactant. Each formulation provides unique advantages depending on the administration route.

Methods: In this study, we aimed to compare three delivery systems with respect to their physicochemical properties such as size and zeta potential, as well as their stability in different physical (temperature) and chemical (pH) conditions. Preliminary studies examining differential permeability and viability after exposure to free CBD and CBD based lipid formulations have been undertaken.

Results: All formulations had an average particle size of less than 250 nm with a polydispersity index below 0.3. All formulations maintained stability at different temperatures, including RT, 4°C and 37°C, except NLC and liposome. Moreover, formulations were stable after exposure to acidic and basic conditions (from pH 2.5 to pH 8.5), except NLC, which showed an increase in particle size at pH 7.4 and 8.5.

Conclusion: We developed a workflow for designing and characterizing lipid-based drug delivery systems for a potential pharmaceutical cannabidiol formulation. We anticipate that results obtained from this study will help to uncover a lead CBD formulation to pursue as a preclinical candidate while providing the framework to develop novel pharmaceutical cannabinoid formulations suitable for human use.

References

- [1] Aparicio-Blanco, J., Sebastián, V., Benoit, J. P., & Torres-Suárez, A. I., *European journal of pharmaceutics and biopharmaceutics*, 2019 134, 126-137.
- [2] Patlolla, R. R., Chougule, M., Patel, A. R., Jackson, T., Tata, P. N., & Singh, M. *Journal of controlled release* 2010 144(2), 233-241.

The antianginal ranolazine fails to improve glycemia and hepatic steatosis in obese liver-specific pyruvate dehydrogenase deficient male mice

Christina T. Saed¹, Seyed Amirhossein Tabatabaei Dakhili¹, Amanda A. Greenwell¹, Jordan S.F. Chan¹, Kunyan Yang¹, Farah Eaton¹, Keshav Gopal¹, Rami Al Batran², John R. Ussher¹

¹Faculty of Pharmacy and Pharmaceutical Sciences, University of Alberta, Edmonton, AB , ²Faculty of Pharmacy, Université de Montréal, Montreal, Quebec

Aims: Non-alcoholic fatty liver disease (NAFLD) increases the risk for obesity-related insulin resistance and type 2 diabetes. Recent studies have demonstrated that stimulating pyruvate dehydrogenase (PDH, gene *Pdha1*), the rate-limiting enzyme of glucose oxidation, can reverse obesity-induced non-alcoholic fatty liver disease (NAFLD), which can be achieved via treatment with the antianginal ranolazine. Accordingly, our aim was to determine whether ranolazine's ability to mitigate obesity-induced NAFLD and hyperglycemia requires increases in hepatic PDH activity.

Methods: We generated liver-specific PDH deficient (*Pdha1*^{Liver^{-/-}}) mice, which were provided a high-fat diet for 12-weeks to induce obesity, whereas their lean controls were fed a low-fat diet. *Pdha1*^{Liver^{-/-}} mice and their albumin-Cre (*Alb*^{Cre}) littermates were randomized to treatment with either vehicle control or ranolazine (50 mg/kg) once daily via oral gavage during the final 5-weeks, following which we assessed body composition, as well as glucose and pyruvate tolerance. Hepatic triacylglycerol (TAG) content was quantified using the Bligh and Dyer method of lipid extraction.

Results: *Pdha1*^{Liver^{-/-}} mice exhibited no overt phenotypic differences (e.g. fat mass, body weight, glucose tolerance) when compared to their *Alb*^{Cre} littermates, though a trend to mild worsening of pyruvate tolerance was observed. Of interest, ranolazine treatment improved glucose tolerance and mildly reduced hepatic TAG content in obese *Alb*^{Cre} mice, but not in

obese *Pdha*^{Liver^{-/-}} mice. The latter was independent of changes in hepatic mRNA expression of genes involved in regulating lipogenesis.

Conclusions/interpretation: Liver-specific PDH deficiency is insufficient to promote an NAFLD phenotype. Nonetheless, hepatic PDH activity partially contributes to how the antianginal, ranolazine, improves glucose tolerance and alleviates hepatic steatosis in obesity.

Impact of the MPE-298 azapeptide ligand of the CD36 scavenger receptor on energy-related myocardial metabolites

Naghme Radmannia^{1, 2}, Liliane Ménard^{1, 2}, David Huynh^{1, 2}, Isabelle Robillard³, William Lubell^{2, 4}, Matthieu Ruiz^{2, 3, 5}, Huy Ong^{1, 2}, Simon-Pierre Gravel^{1, 2}, Sylvie Marleau^{1, 2}

¹Faculty of Pharmacy, ²Université de Montreal, ³Montreal Heart Institute, ⁴Department of Chemistry, ⁵Department of Nutrition

Purpose. Azapeptide analogs of growth hormone-releasing peptides-6 (GHRP-6) have been shown to exert cardiovascular protective properties (Frégeau et al., 2020; Huynh et al., 2018). Following myocardial ischemia-reperfusion (MI/R), changes in cardiac metabolism participate to the onset of cardiac dysfunction and the progression to heart failure. The present study aimed to delineate early changes in myocardial metabolism elicited by MI/R and the effect of the macrocyclic azapeptide MPE-298 as a selective and potent ligand of CD36.

Method. C57BL/6J mice anesthetized with isoflurane were subjected to a transient (30 min) occlusion of the left anterior descending coronary artery (or sham-operated) prior to reperfusion of myocardium for 3 or 24 hours. MPE-298 (Ala-AzapropargylGly-D-Trp-Ala-Trp-D-Phe-Lys(allyl)-NH₂) at a dose of 3 µmol/kg or 0.9% NaCl were injected intravenously 10 min prior to reperfusion. The left ventricle was dissected and assayed for metabolomic analyses by gas chromatography-mass spectrometry.

Results. Hydroxyproline, a marker of fibrosis, was markedly increased after MI/R compared to sham-operated groups at both 3 and 24 hours. Glucogenic amino acids such as arginine, methionine, proline and

asparagine were decreased by MI/R at 3 hours, whereas asparagine was increased at 24 hours in MI/R mice. However, MPE-298, at the dose used, did not affect the left ventricle levels of the amino acids. In our MI/R model, ketone bodies were not affected at either time points, neither were the levels of branched chain amino acids or BCAA (valine, leucine and isoleucine).

Conclusion. We conclude that our MI/R model elicits metabolic changes associated with MI/R injury in mice such as an increase in the hydroxyproline levels and in some glucogenic amino acids. MPE-298, at the dose used, did not change these amino acid levels. This work is supported by a project grant from the CIHR.

References

1. Frégeau et al. *Atherosclerosis* 2020 307: 52-62
2. Huynh et al. *FASEB J* 2018 32: 807-818

Assessing the *in vitro* activity of the pharmaceutically relevant cannabinoids CBD, CBN, and CBG

Brendan Morris-Read¹, Behnoush Kermanshahi¹, Andrea Olaizola², Gokce Alps¹, Thomas Skrinskas³, Jessica Kalra²

¹Langara College, Vancouver, BC, ²University of British Columbia, Vancouver, BC, ³Nanovation Therapeutics, Vancouver, BC

Purpose: Despite the widespread use of Medical Cannabis (MC), there remains a paucity of research assessing the *in vitro* activity of both MC and individual, non-psychoactive, pharmaceutically relevant cannabinoids (PCs) such as Cannabidiol (CBD), Cannabigerol (CBG), and Cannabinol (CBN). This early phase discovery research is essential if PCs are to be considered as potential pharmacotherapies for treating cell perturbations that lead to, or result from, disease.

The studies described herein focus first on solubilization strategies for the PCs CBD, CBG, and CBN, in cell culture media. We subsequently compare their activity *in vitro* using human cervical cancer (HeLa), human liver cancer (HepG2), and human kidney (HEK293T). We hypothesized that CBD, CBG, and CBN have differential cytostatic effects. We further examine the possibility that CBD may behave synergistically with other cytostatic chemotherapies, when used in combination to treat cancer cell lines.

Methods: Cell viability assays were completed in HeLa, HepG2, and HEK293T cells after 24, 48, 72, 96, and 120hr exposure to CBD, CBG, and CBN. CBD and Docetaxel (DTX) were used in combination to determine whether the drugs work synergistically to reduce viability of HeLa cells.

Results: PCs are best solubilized in DMSO before addition to cell culture media. All three PCs demonstrated a dose-dependent decrease in cell viability in all cell lines tested. A synergistic relationship was seen when CBD was used in combination with DTX in HeLa cells.

Conclusion: Each PC had a negative impact on cell viability indicating that these agents are not innocuous to cells. Further examination of PC activity *in vitro* is needed to determine the effects on cell physiology in normal and cancer cell lines. This data will help to uncover appropriate therapeutic targets and support the potential for PCs to be used as pharmacotherapies.

Sex- and Enantiospecific Differences in the Formation Rate of Hydroxyeicosatetraenoic Acids in Rat Organs

Samar Gerges, Ahmad Alammari, Mahmoud El-Ghiaty, Fadumo Isse, Ayman El-Kadi

Faculty of Pharmacy and Pharmaceutical Sciences, University of Alberta, Edmonton, Alberta, Canada

Purpose: Hydroxyeicosatetraenoic acids (HETEs) are hydroxylated arachidonic acid (AA) metabolites that are classified into midchain,

subterminal, and terminal HETEs. Hydroxylation results in the formation of R and S enantiomers for each HETE, except for 20-HETE. HETEs have numerous physiological effects and are implicated in the pathophysiology of several diseases. They are involved in cardiovascular diseases such as hypertension and cardiac hypertrophy, and inflammatory diseases such as diabetic nephropathy and non-alcoholic fatty liver disease. Several studies have demonstrated sex-specific differences in AA metabolism in different organs.

Methods: Microsomes from the heart, liver, kidney, lung, intestine, and brain of adult male and female Sprague Dawley rats were isolated and incubated with AA. Thereafter, enantiomers of all HETEs were analyzed by liquid chromatography-tandem mass spectrometry.

Results: We found significant sex- and enantiospecific differences in the formation rates of different HETEs in all organs. The majority of HETEs, especially midchain HETEs and 20-HETE, showed significantly higher formation rates in male organs. In the liver, the R enantiomer of several HETEs showed higher formation rate than the corresponding S enantiomer (e.g., 8, 9, and 16-HETE). On the other hand, the brain and small intestine demonstrated a higher abundance of the S enantiomer. 19(S)-HETE was more abundant than 19(R)-HETE in all organs except the kidney.

Conclusion: Elucidating sex-specific differences in HETE levels provides interesting insights into their physiological and pathophysiological roles and their possible implications in different diseases.

This work was supported by a grant from the Canadian Institutes of Health Research [CIHR PS 168846] to A.O.S.E-K. S.H.G. is the recipient of Alberta Innovates Graduate Student Scholarship.

In Silico Biopharmaceutics and Activity of Cannabis-Derived Stilbenes

Conor O'Croinin, Andres Garcia Guerra, Raimar Löbenberg, Michael Doschak, Neal M. Davies

¹University of Alberta, Edmonton, AB

Introduction: Polyphenolic stilbenes are known to have therapeutic properties including antioxidant and anti-inflammatory activity. *Cannabis sativa* is a natural source of stilbenes and contains fourteen dihydrostilbenes whose pharmaceutical properties are not well understood. *In silico* predictive modeling can help classify and characterize the pharmaceutical properties of compounds.

Methods: ADMET Predictor 9.5 and Marvin Sketch Chemaxon were used to generate predictive modeling for cannabis-derived stilbenes. The chemical structures of the stilbenes were uploaded into the modeling software, and the metabolism, transporter, and physchem module settings were used to classify and characterize their pharmaceutical properties. Pharmacokinetic data was obtained based on the predictive modeling of the *in vitro* intrinsic clearance in human liver microsomes.

Results: The stilbenes are predicted to be substrates for various cytochrome P450 (CYP) enzymes, with all fourteen being substrates for CYP1A2 and CYP2C19. The cannabis-derived stilbenes inhibited CYP2C9 and showed varying degrees of inhibition against the other tested CYP isoforms. Predictive data for the stilbenes as substrates of UDP glucuronosyltransferase (UTP) showed high potential for glucuronidation of these compounds. The activity of these compounds against HIV-1 integrase was modeled, giving pIC₅₀ values for the stilbenes that range from 3.47 to 4.91. Seven out of the fourteen stilbenes showed predicted inhibition of breast cancer resistance protein. The pharmacokinetic data demonstrated that the half-life of the stilbenes range from 3.94 hours for cannabistilbene IIb to 27.32 hours for HM3. The stilbenes all have a predicted clearance within the range of 12.35 to 36.41 L/h.

Conclusion: The *in silico* predictive modeling of the cannabis-derived stilbenes has provided foundational knowledge about their metabolism, activity, physicochemical properties, and pharmacokinetics. These data

can guide future research into the therapeutic uses of these compounds and the development of formulations. The results suggest that cannabis-derived stilbenes have potential therapeutic applications that warrant further investigation.

Analytical Detection of Cannflavins in Cannabis sativa Extracts and Formulations

Conor O'Croinin, Tyson S. Le, Andres Garcia Guerra, Raimar Löbenberg, Michael Doschak, Neal M. Davies

¹University of Alberta, Edmonton, AB

Introduction: *Cannabis sativa* is known to contain more than 550 different compounds. The isolation, detection, and quantification of these compounds are crucial for future research and product development.

Methods: This study developed a selective and sensitive liquid chromatography mass spectrometry assay to detect several cannflavins in hemp extracts. The mobile phase consisting of acetonitrile and water with 0.1% formic acid [83:17] was used, and detection was carried out by electrospray positive ionization in single-ion monitoring mode through a C-18 analytical column. The deuterated analog cannabidiol-D3 was used as an internal standard. A topical formulation was developed and the release of cannflavins from this formulation across a synthetic hydrophobic membrane was investigated using Franz diffusion cells.

Results: The calibration curve was linear for all three cannflavins in the range of 0.5 µg/mL to 2.5 µg/mL ($r^2 \geq 0.992$), with a lower limit of quantification of 0.5 µg/mL and a limit of detection of 0.25 µg/mL. The method was stable under various conditions, and the intra- and inter-assay precision had less than 20% variation. The results showed that the topical formulation had a more effective release of cannflavins than a commercial product releasing diclofenac.

Conclusions: The developed methodology and initial formulation development lay the foundation for further research into cannflavins and

other poorly understood cannabis-derived compounds. With excellent linearity and suitable measures of stability, sensitivity, and selectivity, this assay is a valuable tool for the detection and quantification of cannflavins in various specimen types. The development of this methodology and the initial formulation development sets the foundation for further pharmaceutical research into these compounds.

Microwave-induced transient heating accelerates protein PEGylation

Ahlem Meziadi¹, Andrea A Greschner¹, Marc A Gauthier¹

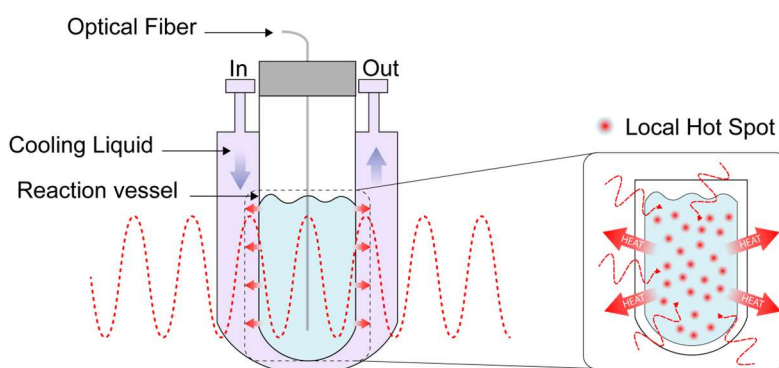
¹Institut National de la recherche Scientifique (INRS), Varennes, Québec, Canada

Purpose: The poor efficiency of the PEGylation reaction generally implies that a significant excess of mPEG is used.[1] This drives up the cost of producing a given mPEG-protein bioconjugate and complicates purification.[2,3] In this work, we focused on enhancing protein PEGylation.

Methods: A novel strategy for protein PEGylation by transient heating of the solution using a simultaneously-cooled microwave (MW) reactor was investigated to promote the interaction between mPEG and proteins. The MW reactor operates at a frequency of 2.45 GHz and can keep constant bulk reaction temperatures of ~25°C while the reaction mixture is exposed to MW irradiation.[4]

Results: Microwave-induced transient heating phenomenon can be exploited to accelerate protein PEGylation significantly and even increase the degree of PEGylation achievable beyond what is possible at room temperature. This can be accomplished under conditions that do not compromise protein integrity. Several PEGylation chemistries and proteins are tested, and mechanistic insight is provided. Under certain conditions, extremely high levels of PEGylation were achieved in a matter of minutes. Moreover, considering the significantly reduced reaction times, the microwave-induced transient heating concept was adapted for continuous flow manufacturing of bioconjugates.

Conclusion: Overall, this study demonstrates that transient heating had a pronounced positive effect on the rate of multiple types of PEGylation reactions, presumably via transient thermal enhancement of molecular dynamics that increase the availability of the reactive groups on the macromolecules. Proteins were not denatured under most conditions examined, and very high degrees of PEGylation was obtained in minutes under certain circumstances. This concept seems most appropriate for slow PEGylation reactions (reductive alkylation, Michael addition), and can be adapted to produce bioconjugates in a flow reactor setting for scaling-up.



References

- [1] Chem. Soc. Rev. 2018 47: 8998-9014
- [2] J. Pharm. Sci. 2003 92: 97-103
- [3] Biotechnol. J. 7:2012: 592-593
- [4] J. Am. Chem. Soc. 2019 141: 3456-3469"

Anti-Viral and Anti-Inflammatory Effects of novel PPAR γ Agonist, INT131 in the context of HIV-Associated Neurocognitive Disorders

Celene Titus, Hoque Tozammel, Reina Bendayan
 University of Toronto, Toronto, Ontario

Background: Approximately 50% HIV-infected individuals develop HIV-associated neurocognitive disorders (HAND), manifested by declined motor/cognitive functions. Activation of peroxisome proliferator-activated receptor gamma (PPAR γ), a transcription factor known to regulate glucose/lipid metabolism can also exert anti-HIV/anti-

inflammatory effects¹. We hypothesized that PPAR γ activation by a novel agonist, INT131, could suppress HIV-associated brain inflammation *in vivo*, in an ecotropic HIV-1 (EcoHIV) mouse model representative of HAND^{1,2}. The goal of this study was to examine the role of INT131 in reversing infectivity and inflammation in brain cerebellum, subcortical and cortical regions in EcoHIV infected mice.

Methods: Using qPCR, we have quantified markers for viral genes, inflammatory cytokines/chemokines, blood-brain barrier (BBB) tight-junction proteins, and examined BBB permeability applying the NaF permeability assay, 21 days post intracranial injection of saline or EcoHIV (2×10^8 pg/ml) in: i) non infected mice, ii) infected EcoHIV mice, and iii) infected EcoHIV mice treated with daily oral administration of INT131 (50 mg/kg/day). To analyze the anti-viral effects of INT131, we are currently assessing viral DNA 2LTR and EcoHIV gag via qPCR and measuring p24 via immunohistochemistry to determine the localization of viral protein in the brain.

Results: Compared to saline injected controls, exposure of mice to EcoHIV, significantly increased the mRNA expression of viral genes (*Vif* and *Tat*), inflammatory markers (*Tnf- α* , *Il-1b*, *Il-6*, and *Ifn- γ*) and decreased BBB markers (*Ocln*, *Cldn5* and *Tjp-1*) in brain regions. INT131 significantly reduced the expression of inflammatory markers and restored the expression of BBB markers to control levels. We also observed a restoration of BBB permeability *in vivo*, measured by NaF assay, with INT131 treatment.

Conclusion: Our work revealed that PPAR γ could constitute a potential target for the treatment/prevention of HIV-1 associated brain inflammation, BBB dysfunction and/or HAND. Future behavioural studies will investigate the efficacy of INT131 in reversing neurocognitive deficits in the EcoHIV mouse model.

References

1. FASEB J 2020 34 (2): 1996-2010
2. PLOS J 2018 14(6): e1007061

Adverse drug reactions to PEGylated drugs: preclinical evidence and novel mitigation strategies

Kevin Coutu¹, Andrea Greschner¹, Marc Gauthier¹, Nicole Drossis^{1, 2},
Nicolas Bertrand³

¹INRS, ²Ontario Tech University, ³CRCHUL-Quebec

Background: Modification of therapeutic proteins with poly(ethylene glycol) (PEG), called PEGylation, is one of the most common approaches to increase their stability and prolong their life in the bloodstream. In fact, one of the advantages of PEGylation is to mask the epitopes of non-human proteins to the immune system. To date, research has focused primarily on the biophysical aspects of PEGylation and has paid much less attention to the clinical challenges associated with PEG exposure.

One possible solution is to develop a biodegradable PEG whose properties would change over time. If designed appropriately, biodegradable PEG coatings could provide fluidity to the types of epitopes exposed during circulation and provide a means to achieve removal rather than accumulation in peripheral tissues. This presentation will provide an overview of the strategies that could be used to achieve these effects as well as the clinical opportunities they offer.

Methods: 3 drug candidates were selected for *in vitro* PK/PD from a library of 18 L-Asparaginase bioconjugates based on their immunogenicity measured by indirect ELISA, their enzymatic activity compared to the native form and their size by Dynamic Light Scattering.

Results: The corresponding "biodegraded" ASNase bioconjugate, with only short side chains, retains its activity (20% compared with native ASNase), but has retained its very low antigenicity (<0.1%) and, more importantly, has a DH<10 nm, which should allow glomerular filtration. Our preliminary results show that _{comb}PEG-ASNase and Biodegradable-ASNase, with the same initial sizes, exhibit very different PK/PD profiles over a 7-day period in Balb/c mice.

Conclusions: Overall, these will lead to better tolerated treatments and a better understanding of how to manage at-risk children and adolescents with anti-PEG antibodies. We will also confirm whether alternative polymeric conjugates based on _{comb}PEG or Biodegradable PEG are a viable solution for biodegradable drug delivery system.

Macrophage-Modulating Polymers for Local Delivery of Cancer Immunotherapeutics

Michael Celejewski^{1, 2}

¹McMaster University, ²NSERC CREATE Controlled Release Leaders (ContRoL)

Purpose: Despite the potential of cancer immunotherapies, efficacy is often hindered for many solid tumors, such as glioblastoma (GBM), due to transport barriers and therapy suppressive tumor-associated macrophages (TAMs). Bioactive hydrogels implanted into tumor resection cavities could overcome transport barriers and increase the ratio of pro-inflammatory (M1) to anti-inflammatory (M2) macrophages to support therapies (Figure 1a, 1b). We are designing degradable hydrogels with polymers incorporating the RP-182 peptide (KFRKAFKRFF) for TAM depletion and repolarization towards M1-like TAMs, for applications involving local immunotherapeutic delivery (Figure 1c).

Methods: *i) Local delivery within a multicellular spheroid model.*

poly(carboxybetaine) (pCB) hydrogels modified with neutravidin were used to control the release of a T cell Engager, D-DATE, in a multicellular model incorporating GBM spheroids and T cells. Spheroid size was tracked upon D-DATE administration.

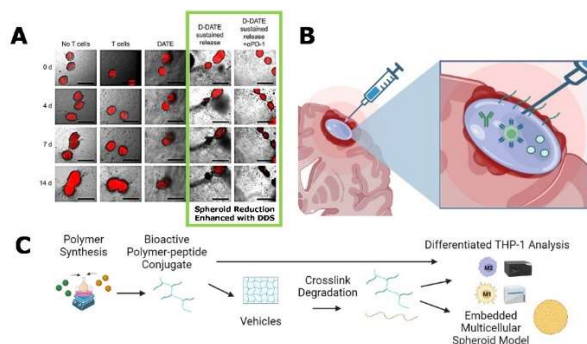
ii) Conjugate and gel formation. Bio-inert pCB-dibenzocyclooctyne N-hydroxysuccinimide) (pCB-DBCO) copolymers are being synthesized and conjugated to an azide-modified RP-182 peptide. For tunable hydrogel degradation, a pCB-azide polymer with tunable hydrolytic carbamate

bonds will be synthesized. The peptide-polymer conjugate will crosslink with pCB-azide to form the hydrogel. In polarized THP-1 monocyte derived macrophage cultures, depletion will be tracked using cell viability assays with alamarBlue fluorescence. Repolarization will be tracked by flow cytometry and cytokine quantification.

iii) 3D cell-culture model. The TAM-modulating gel will be screened with embedded multicellular spheroids in the presence and absence of cancer drugs. Spheroid size and cytokine levels will be tracked to evaluate TAM activities.

Results: Using displacement affinity release, we have previously demonstrated that the local and sustained delivery of D-DATE from pCB hydrogels within multicellular spheroid models improved spheroid killing over extended timepoints compared to a single D-DATE administration (Figure 1a).

Conclusion: Injectable macrophage-modulating hydrogels will aid in modulation of tumor microenvironments to improve the efficacy of local drug delivery vehicles for immunotherapeutics against solid tumors.



References

- [1] Sci Transl Med. 2020 12: eaax6337
- [2] J Control Release 2022 338: 386-396

Inhalable Yeast Beta-Glucan Microparticles Prepared by Pressurized Gas eXpanded (PGX) Liquid Technology for the Treatment of Fibrotic Lung Diseases

Nate Dowdall¹, Safaa Naiel¹, Spencer Revill¹, Quan Zhou¹, Pareesa Ali¹, Aaron Hayat¹, Vaishnavi Kumaran¹, Javad Mahmoudi², James Hu², Emily Wong², Ricardo Couto², Byron Yépez², Bernhard Seifried², Paul Moquin², Myrna Dolovich¹, Rod Rhem¹, Martin R. Kolb¹, Kjetil Ask¹, Todd Hoare¹

¹McMaster University, Hamilton, ON, ²Ceapro Inc., Edmonton, AB

Background: Pulmonary fibrosis (PF) is a condition in which excessive scarring of the lungs causes a severe reduction in lung function. Pro-fibrotic macrophages play a key role in initiating and progressing PF due to their ability to secrete pro-fibrotic cytokines and produce extracellular matrix. Although recently approved anti-fibrotic drugs have improved patient prognosis, these current treatments induce systemic toxicity and are unable to fully halt or reverse fibrotic progression.

Yeast beta-glucan (YBG), a polysaccharide derived from *Saccharomyces cerevisiae*, is a well-known macrophage immunomodulator. YBG can activate the Dectin-1 receptor expressed on macrophages and convert pro-fibrotic macrophages to an anti-fibrotic phenotype¹. However, current commercial/conventional extraction and drying methods lead to variable/inconsistent physical and biological properties of YBG, thereby limiting YBG's potential as an immunomodulatory therapeutic.

Methods: YBG microparticles were prepared using Ceapro Inc.'s Pressurized Gas eXpanded (PGX) liquid technology. PGX-YBG was compared to commercially available YBGs in terms of size, morphology, density, porosity, and Dectin-1 activation. PGX-YBG was tested *in vitro* and in *ex vivo* murine lung slices for modulation of macrophage phenotype markers. PGX-YBG powders were characterized for inhalability using the Next Generation Impactor.

Results: Relative to commercial YBGs, PGX-YBG exhibited a smaller, monodisperse size distribution, with >90% of microparticles smaller than 8 μm . PGX-YBG exhibited a high specific surface area ($132 \pm 5 \text{ m}^2/\text{g}$) and low bulk density ($0.073 \pm 0.01 \text{ g/mL}$), characteristics that are conducive to highly respirable particles. Aerosolization experiments indeed indicated that PGX-YBG could effectively reach the deep lung where fibrosis occurs. Finally, PGX-YBG exhibited potent Dectin-1 activation and was shown to prevent pro-fibrotic macrophage polarization *in vitro* and in *ex vivo* lung slices.

Conclusion: PGX-YBG has the potential to be delivered directly to the lung, prevent systemic toxicity, and inhibit macrophage-directed fibrosis.

References:

Y. Su, L. Chen, F. Yang, P. Cheung. Carbohydrate Polymers 2021:117258
Carbohydrate Polymers 2021 253: 117258

A modular platform for rapidly optimizing the structure of bispecific antibodies using DNA nanotechnology

Sabrina Messaoudi¹, Marc A Gauthier¹, Yves Durocher², Andrea Greschner¹, Ryan Wylie³

¹Institut national de la recherche scientifique INRS-EMT, Varennes, QC,
²National Research Council Canada CNRC-NRC, Montreal, Qc, ³McMaster University, Hamilton, ON

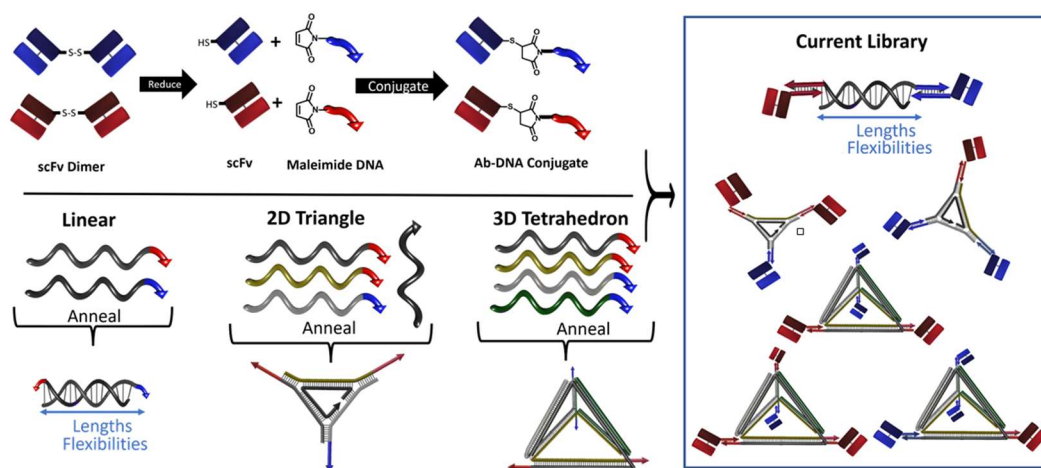
Purpose: Bispecific antibodies (bsAb) have shown promise in cancer treatment as they can kill cells by binding two targets simultaneously, such as a cancer cell and a cancer-killing T-cell.¹ However, a major challenge in bsAb development comes from the largely unknown way cells ‘display’ their antigens. That is, epitopes can be in crowded locations on the antigen or in highly exposed ones. As such, it is presently unknown what the optimal design of a bsAb should be for productive T-cell engagement. To address this challenge, a modular bsAb platform has been designed that uses DNA nanotechnology to determine the optimal distance between the antigen-binding domains of a known bispecific, blinatumomab², the benefit of structural flexibility between antibodies, as well as the effect of increasing the number of antigen binding domains.

Methods: A library of DNA-based hybrid antiCD19/antiCD3 bsAb with varying inter-antibody distance, flexibility and the number of appended antigen-binding units was created. Combinations of short custom DNA oligonucleotides were designed. ScFv antibody fragments were conjugated to the DNA oligonucleotides, which permitted controlled assembly of the hybrid bsAb structures. To validate their efficacy, lysis of

CD19+ cells by T-cells was measured *in vitro*.

Results: ScFv production in CHO cells was confirmed via PAGE and contained both monomeric and dimeric species. Two scFv monomers were successfully conjugated to DNA-maleimide. Assembly of a library of 14 linear bispecific structures of varying size and flexibility and 5 2D and 3D structures varying the relative number of scFv fragments was confirmed via PAGE. *In vitro* tests of bsAb structures with cancer cells and T-cells shows a rapid and efficacious cell lysis, better than the clinically used blinatumomab.

Conclusion: DNA nanotechnology provided a modular framework for quickly creating a library of bsAb with different physical characteristics and revealed parameters by which bsAb design can be improved.



References

- (1) Science 2021 372 (6545): 916-917.
- (2) Clinical Oncology 2019 29 (18): 2493-2498.

Studying the Aryl Hydrocarbon Receptor Conformational Changes in the Presence of AhR Modulators

Farag Mosa, Ayman El-Kadi, Khaled Barakat

¹University of Alberta

Purpose: The aryl hydrocarbon receptor (AhR) is an environmental sensor that combines metabolic and biological inputs to regulate complex cellular responses. It controls the expression of several genes, such as cytochrome P450 (CYP) 1A1, 1A2 and 1B1. It has a pathophysiological role in a variety of disorders, including tumor growth, cardiovascular disease, and viral infection. AhR modulator (agonists/antagonists) induce conformational and structural changes in several domains in the AhR structure. Here, we used a combination of classical molecular dynamics (MD) simulations and enhanced sampling algorithms to understand how the binding of AhR ligands can induce dynamical changes to the AhR structure

Methods: 3D structures of human AhR were built using the Alphafold artificial intelligence (AI) tool. Three AhR models involving two ligand-bound models and apo AhR structure were selected and validated using MD simulations, followed by clustering analysis to extract their most dominant conformations. The binding free energy of each ligand was then calculated, and enhanced sampling methods were used to accurately portray the free energy landscapes for all systems

Results: selected models had root mean square deviation (RMSD) around 0.770 angstroms compared to the reference crystal structure. Additionally, their Ramachandran plot indicated that more than 93% of residues were in the favoured region and less than 1% were in disallowed region. The top conformations in each model were determined through clustering analysis. After completing binding free energy calculations using the initial 50 ns MD trajectory, the best docked poses were selected. Furthermore, essential conformational changes in two regions of AhR were detected.

Conclusions: When AhR ligands bind to the PAS-B domain, structural changes in AhR occur. These changes are critical in the transfer of AhR from inactive to active mode. Our results pave the way for a more in-depth knowledge about AhR activation and inhibition at the atomic level.

Lipid nanoparticle screening for gene replacement therapy

Nassim oumansour¹, Matthias Zadory¹, Grégoire Leclair¹, Davide Brambilla¹

¹University of Montreal, Montreal, QC

Lipid nanoparticles (LNPs) have been successfully utilized for Messenger RNA (mRNA) delivery in COVID-19 vaccines, demonstrating the potential of nanotechnology as nucleic acid delivery tools. LNPs consists of four components - ionizable lipid, phospholipid, cholesterol, and polyethylene glycol. The relative ratios of these components can significantly affect mRNA delivery and protein expression. In this study, we used a Design of Experiment (DOE) approach to optimize LNP formulations for in vitro mRNA delivery of lysosomal acid lipase (LAL) mRNA. LAL is a key enzyme that hydrolyses cholesteryl esters and triglycerides. We systematically varied the molar ratio of the four components and the identity of the ionizable lipid and phospholipid. We characterized the formulations using physicochemical parameters including size, polydispersity, encapsulation efficiency, and surface charge. We performed statistical analysis to understand the relationship between physicochemical properties and mRNA delivery. A selected set of formulations were evaluated in an in vitro knockdown model of LAL in hepatocytes to assess the efficiency of LAL mRNA delivery and restoration of enzymatic activity. Rescue experiments with mRNA-LNPs showed a dose-dependent increase in protein expression, with a maximum increase of 800% in LAL enzymatic activity 24 hours post-transfection, followed by a sharp decline until 72 hours. Notably, four formulations demonstrated a protein expression increase of at least 400% with Western blot and qPCR analyses confirming the observed increase. More specifically, formulations with the phospholipids DSPC and HSPC yielded the highest mRNA-induced LAL expression showing a new insight into the importance of the helper lipids in achieving high efficacy in delivery. Our approach successfully optimized the delivery of LAL mRNA, offering a promising therapeutic strategy for LAL deficiency and can be extended to other diseases that require targeted mRNA delivery. Overall, our study highlights the potential of LNPs and their composition for the effective delivery of mRNA-based therapies.

References

(1) Nanoscale 14.4 (2022): 1480-1491.

(2) Biomaterials science 9.4 (2021): 1449-1463.

Emerging approaches to detect analytes of interest in complex biological matrixes

Tazib Rahaman Syed, Andrea Greschner, Marc Andre Gauthier
INRS-EMT, Montreal QC

Abstract: ELISA is one of the most common tools to detect molecules of interest in the biosciences. This assay is laborious, multi-stepped, and uses expensive reagents. Other techniques, such as surface plasmon resonance and polymerase chain reaction, can suffer from scalability issues, poor selectivity, errors, sample contamination, and the use of expensive equipment. Nucleic-acid based aptamers are stable and inexpensive analogues of antibodies that can be used as recognition elements for specific analytes. Nucleic acid nanostructures can also sometimes display chemical properties that could be useful for detection purposes. This presentation begins by summarizing the analytical techniques most commonly used to detect analytes within complex biological matrixes, and their shortcomings. Thereafter, it presents emerging approaches to address these challenges using DNA nanotechnology.

References

1. Liu, X., Yan, H., Liu, Y., & Chang, Y. (2011). Targeted cell-cell interactions by DNA nanoscaffold-templated multivalent bispecific aptamers. *Small (Weinheim an der Bergstrasse, Germany)*, 7(12), 1673-1682. <https://doi.org/10.1002/sml.201002292>
2. Kolarevic, A., Pavlovic, A., Djordjevic, A., Lazarevic, J., Savic, S., Kocic, G., Anderluh, M., & Smelcerovic, A. (2019). Rutin as Deoxyribonuclease I Inhibitor. *Chemistry & biodiversity*, 16(5), e1900069. <https://doi.org/10.1002/cbdv.201900069>

Recrystallization Inhibition of Celecoxib by a Novel Polymeric Nanogel in Controlled Release Amorphous Solid Dispersion Beads: Experimental Studies and Molecular Dynamics Analysis

Jamie Anne Lugtu-Pe¹, Xuning Zhang¹, Sako Mirzaie¹, Hao Han R. Chang¹, Nour AL-Mousawi², Kuan Chen¹, Anil Kane³, Daniel Bar-Shalom², Xiao Yu Wu¹

¹University of Toronto, ²University of Denmark, ³Thermo Fisher Scientific

Purpose Controlled release amorphous solid dispersion (CRASD) is a promising strategy to elevate the solubility of the ubiquitous poorly soluble drugs over prolonged duration¹. However, like other supersaturating systems, drug recrystallization within the dosage form is a challenge. Recently, we have developed a non-leachable terpolymer nanoparticle (TPN) with superior coating processability and pH-dependent swellability as a film-coating pore former². Herein, we utilized these unique features and potential drug-polymer interactions to explore this polymeric nanogel as an internal recrystallization inhibitor and investigated its impact on maximizing the drug release extent and duration as compared to a conventional pore former, polyvinylpyrrolidone (PVP).

Method CRASD beads containing a celecoxib reservoir and insoluble polymer (ethylcellulose, EC) membrane were prepared with either TPN or PVP as pore formers by fluid-bed coating. Dissolution studies were conducted over 24 h and the beads were examined using SEM and polarized light microscopy. Molecular dynamics (MD) simulation was performed to elucidate the role of molecular interaction on recrystallization inhibition.

Results CRASD formulations provided extended release up to 24 h, with 4 to 6x higher extent and C_{max} than crystalline celecoxib. Formulations containing TPN achieved ~12% higher AUC levels compared to those with PVP ($p < 0.01$) and remained more intact with less birefringence, a measure of internal crystallization. Formulations with PVP exhibited greater birefringence, accompanied by leaching, evidenced by visible ruptures at 5 h. MD analyses revealed a lower degree of intra-molecular bonding, crystal formation, diffusion coefficient, and molecular flexibility of celecoxib in presence of TPN compared to PVP, attributable to enhanced intermolecular H-bonding between celecoxib and TPN.

Conclusion The results suggest that a polymeric nanogel with non-leachability and strong molecular interaction with drug molecules can serve as a superior pore former in a coated CRASD bead to maintain membrane integrity and permeability and inhibit internal recrystallization of poorly soluble drugs.

References

1. Mol Pharm 18.11 (2021): 4198-4209.
2. Eur J Pharm Biopharm 120 (2017): 116-125.

Methylmercury Induces The Detoxifying Enzyme NAD(P)H: quinone oxidoreductase 1 Via a Transcriptional Mechanism in Hepa-1c1c7 Cells

Mohammed Alqahtani, Mahmoud El-Ghiaty, Ayman El-Kadi

Faculty of Pharmacy and Pharmaceutical Sciences, University of Alberta

Mohammed A. Alqahtani, Mahmoud A. El-Ghiaty and Ayman O.S. El-Kadi

Faculty of Pharmacy and Pharmaceutical Sciences, University of Alberta,
Edmonton, Alberta, Canada

Purpose: Methylmercury (MeHg) has been reported to induce a battery of antioxidant enzymes including NAD(P)H: quinone oxidoreductase 1 (NQO1) which plays a key role in the cellular protection against oxidative stress and cancer prevention¹. The nuclear factor erythroid 2-related factor-2 (NRF2) and aryl hydrocarbon receptor (AHR) are the two transcription factors that regulate the NQO1 expression. This co-regulation prompted us to investigate which transcription factor is involved in the modulation of NQO1 expression in response to MeHg exposure.

Methods: Murine hepatoma Hepa-1c1c7 cells were treated with increasing concentrations of MeHg (1.25, 2.5 and 5 μ M) in the absence or presence of NQO1 inducer, 2,3,7,8-tetrachlorodibenzo-*p*-dioxin (TCDD). The NQO1 expression was assessed at mRNA and protein levels using RT-qPCR and Western blot, respectively. NQO1 activity was measured via a fluorescence-based assay. Transfected Hepa-1c1c7 cells were utilized for evaluating AHR- and NRF2-dependent luciferase

reporter assays.

Results: MeHg induced NQO1 mRNA, protein, and activity in a concentration-dependent manner. Additionally, MeHg increased the nuclear accumulation of NRF2, but not AHR, in a time-dependent manner. Also, NRF2-driven luciferase activity was induced by MeHg, while that of AHR was unchanged.

Conclusion: This study demonstrates that MeHg up-regulates the expression of the detoxifying enzyme NQO1 at a transcriptional level in Hepa-1c1c7 cells via NRF2-dependent mechanism.

References

BMB reports 2015 48: 609

Functionalized nanodiamonds as gene delivery agents: Biocompatibility and biodistribution

Saniya Alwani, [Iulia Spataru](#), Eiko Kawamura, Deborah Michel, Ildiko Badea

University of Saskatchewan, Saskatoon, SK, ²Western College of Veterinary Medicine Imaging Centre, University of Saskatchewan, Saskatoon, SK

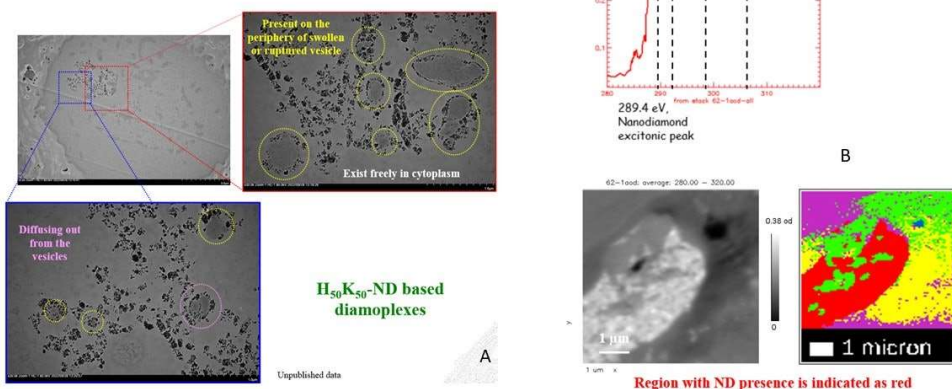
Purpose: Oncogenes have been explored as therapeutic targets for hepatic tumors. Myeloid cell leukemia-1 (MCL-1) gene is overexpressed in half of hepatic malignancies, and potential target for nucleic acid therapy. One of the fundamental quests in nucleic acid delivery is to overcome the cellular and molecular barriers of nucleic acid transfer. The aim of this research is to design and evaluate amino acid-functionalized nanodiamonds (NDs) as delivery vectors for nucleic acids. NDs, the most biocompatible carbon-based particles, are versatile platforms for building nucleic acid complexes (diamplexes). To serve this purpose, we utilized amino acid-functionalized nanodiamonds (fNDs) as small interfering ribonucleic acid (siRNA) carriers, diamplexes against this oncogene.

Methods: Three types of fNDs: lysine-NDs (K-NDs); lysyl-histidine-NDs (HK-NDs) and lysine/lysyl-histidine-NDs (H₅₀K₅₀-NDs) were synthesized. fNDs were conjugated to siRNA and used to knock down MCL-1 expression in hepatocellular carcinoma model.

Results: All fNDs maintained cell viability of more than 70% up to 100 µg/mL, a concentration at least double than the effective concentration used in subsequent bioassays. H₅₀K₅₀-NDs displayed a different mechanism of internalization¹, macropinocytosis, and improved capacity to escape endo-lysosomal compartments as opposed to K-NDs and HK-NDs², demonstrated by transmission electron microscopy (Figure 1A) and synchrotron-based scanning x-ray microscopy (Figure 1B).

Conclusion: Overall, this work shows that fND-based diamoplexes are a novel treatment strategy for hepatic tumors, due to their, optimum intracellular distribution and high degree of bio-safety.

Figure 1. TEM (A) and STXM (B) images corresponding to the same cell confirming intracellular distribution of H50K50-based diamoplexes in HepG2 cells, along with X-ray absorption spectrum showing diamond sp3 characteristic peaks.



References

1. Diam Rel Mater 2019 98, 107477.
2. Pharmaceutics 2022 14(9), 1794.

Evaluating the antibacterial and wound healing promoting effects of PVP/PVP-I containing liquid scaffold in vitro and in vivo.

**Samin Abbasidezfouli¹, Aziz Ghahary², Nafise Amiri², Sahand Ghaffari¹,
Ida Hassanpour², Ruhangiz Kilani², Dirk Lange¹**

¹The Stone Centre at Vancouver General Hospital, Department of Urologic Sciences, University of British Columbia, Vancouver, Canada,

²Professional Fire Fighter's Burn and Wound Healing Research Laboratory, Division of Plastic Surgery, Department of Surgery, University of British Columbia, Vancouver, Canada

Purpose: Based on the WHO report in 2018, 11 million burn injuries occur worldwide annually, 180,000 of which are lethal. Over the past few years, many studies have demonstrated that infection and delayed wound healing are responsible for 42%-65% mortality in burn victims. Mesh Fill is a nutritional liquid scaffold found to improve wound healing and esthetic outcomes upon application in a split-thickness meshed skin graft (STMSG) in a porcine model. To expand the efficacy of MeshFill and address the prevention of infections due to wound contamination, our group added antimicrobial properties by replacing polyvinyl alcohol (PVA), a component in the MeshFill complex, with Povidone-iodine (PVP-I). The aim of this study was to develop an antibacterial nutritional liquid scaffold which can be used in full-thickness wounds to reduce the infection rate and accelerate wound healing.

Method: We assessed the antibacterial effect of various ratios of PVP-I/PVP scaffold on both gram-positive and gram-negative bacteria during the 4- and 24-hour time points. The cytotoxicity of the three best ratios of PVP-I/PVP scaffold was assessed on fibroblasts using the live and dead assay while the full-thickness wound epithelialization in terms of antibacterial activity and subsequent healing was evaluated in Sprague Dawley (SD) rats using CFU counts from tissue and histological analyses.

Result: In terms of antibacterial activity, 150% and 200% PVP-I/PVP scaffold was shown to kill gram-positive and gram-negative species most effectively compared to other groups. Moreover, 100% and 150% PVP-I/PVP scaffold showed the best healing results in vivo and did

not delay the healing process.

Conclusion: Scaffoderm containing 150% PVP-I/PVP is most efficacious in terms of antibacterial activity in full-thickness wounds and the promotion of wound healing. The incorporation of PVP-I into MeshFill may be an effective method to prevent impaired wound healing caused by bacterial infection.

Design of Microneedles for Non-Invasive Administration of Sustained Release Anti-Psoriatic Formulations

Fatma Moawad¹, Yasmine Ruel², Roxane Pouliot², Davide Brambilla¹

¹Université de Montréal, Montréal, Québec , ²Université Laval, Québec, Québec

Psoriasis is a chronic skin condition that requires long-term management, for which the transdermal route has great preference owing to accessibility and ease of administration. Besides, sustained-release formulations offer extra advantages by reducing the administration frequency. Together, transdermal administration of sustained-release formulations could greatly improve patients' compliance and hence the net therapeutic outcome. Here, we report the development of microneedle patches with separable, slowly degrading tips for the sustained delivery of different anti-psoriatic medications for the long-term control of the disease; namely "methotrexate" as a reference standard for psoriasis management and the natural compound "phloretin" as a potentially *safer* alternative to methotrexate. Both compounds exhibit strong anti-inflammatory, immunosuppressive, and antiproliferative properties [1, 2]. The patches are made entirely from biocompatible polymers and the separable tips are made mainly from the poly(lactic-co-glycolic) acid copolymer. The needles showed high mechanical strength (≥ 25 N/Patch) with more than 90% needles' penetration and tips' detachment efficiency, only 5 minutes post application to rat skin (ex vivo). Histology sections of the skin showed ~ 120 μm penetration depth of the developed 500- μm needle, ensuring high drug content at the active sites of the disease.

Both drugs have been loaded successfully in considerable amounts in these biodegradable tips (140 µg/patch) with good stability. Both drugs exhibited extended-release profiles over a few days ($\leq 70\%$ cumulative drug release within 48 h), the tips retained most of their size and shape over a 3-week period under similar physiological conditions. The anti-psoriatic efficacy of these patches will be tested both in vitro and in vivo in a psoriasis-like mice model.

The developed patches serve as an efficient pain-free alternative to the current oral and subcutaneous forms of the drugs under study. Furthermore, these patches offer a patient-friendly platform for the delivery of a variety of compounds for therapeutic, diagnostic, and immunological purposes.

References

1. Griffiths, C., et al., Psoriasis. *Lancet*, 2021. 397(10281): p. 1301-1315.
2. Zhang, X., et al., Smart microneedles for therapy and diagnosis. *Research* 2020. 2020: p. 26.

Blood glutamate scavenging: Invoking homeostasis to protect the brain from glutamate excitotoxicity

Ahlem Zaghmi¹, Antonio Dopico-Lopez², Maria Perez-Mato^{2, 3}, Ramon Iglesias-Rey², Pablo Hervella², Andrea A Greschner¹, Ana Bugallo-Casal², Jose Castillo², Francisco Campos Perez², Marc A Gauthier¹

¹Institut National de la Recherche Scientifique, Varennes, Qc, ²IDIS, Santiago de Compostela, Spain, ³Universidad Autonoma de Madrid, Madrid, Spain

Glutamate is an important neurotransmitter, and is particularly involved in memory and learning. Excessive glutamate, however, has an excitotoxic effect and has been linked to many neurodegenerative diseases, including ALS, Alzheimer's, and ischemic stroke. As such, reducing glutamate brain concentration has been a target for therapeutic development, but has been hampered by a several challenges: 1) no

extra-synaptic enzymes exist for its degradation; 2) concentration is dependent on cellular fast uptake by transporters; 3) the blood-brain barrier (BBB) interferes with drug delivery. Efforts to directly target glutamate receptors in the brain have resulted in serious side effects. Here, an alternative approach is used to manage brain glutamate concentration. Ischemic rats were chosen as a model due to the reproducibility of infarcts and resulting increases in glutamate levels. PEGylated glutamate oxaloacetate transaminase (GOT) was synthesized and injected intravenously. Treatment of rats with transient focal ischemia using PEG-GOT produced positive results both in terms of limiting the infarct size and limiting functional impairment. Importantly, it was not necessary to target or cross the BBB with PEG-GOT to observe these effects. Instead, a scavenging effect is suspected where decreases in blood glutamate invoke the natural mechanisms of glutamate transport out of the brain, re-establishing homeostasis. This offers an intriguing approach to treating brain-based illnesses.

References

Commun Biol. 2020 3: 729

Development and validation of a high throughput ultra-performance liquid chromatography assay for the simultaneous determinations of *p*-cresol and its major metabolite *p*-cresyl sulfate in hepatoma cell culture

Ala'a Al Dajani, Qi Kun Hou Hou, Yan Rong¹, Tony Kiang

University of Alberta, Edmonton, AB

Purpose: *p*-Cresyl sulfate (*p*CS), the major sulfonated metabolite of *p*-cresol (*p*C), is a uremic toxin accumulated to high concentrations in patients with impaired kidney function. Both *p*C and *p*CS are associated with the pathophysiology of organ (e.g., liver and kidney) toxicities. The present work describes the development of an analytical assay capable of simultaneously measuring both *p*C and *p*CS in HepaRG tissue culture for toxicokinetic studies.

Methods: Instrumentation consisted of the Shimadzu LC-2040C Plus ultra-high performance liquid chromatography (UPLC) fitted with Agilent Eclipse XDB-C18 column (5 μ m particle size, 4.6mm inner diameter, 250mm length). 2, 6-Dimethylphenol was the internal standard. Using the previously determined excitation (268nm) and emission (300nm) wavelengths for fluorescence detection, the following assay parameters were optimized in HepaRG culture medium: i) ratio of sample: acetonitrile (ACN) for extraction and protein precipitation, ii) sample clean up (i.e., incubation, centrifugation, freeze-drying), iii) water: ACN ratio in the mobile phase (with 0.8mM ammonium acetate and 0.1% formic acid), and iv) flow rate.

Results: Using optimized conditions [i) 1:6 sample: ACN for extraction; ii) 20min incubation at 25°C, centrifugation at 18600g for 20min at 4°C, freeze-drying for 2min at 45°C, and further incubation at -20°C for 60min; iii) 40% water; iv) 0.3mL/min flow rate for 16min, 1mL/min for 5min, then 0.3mL/min for 2min for a run time of 25min], 10 μ L of sample was injected into the UPLC. Retention times were 11.4min and 8.2min, whereas calibration ranges were 1.16-35 μ g/mL and 1.86-35 μ g/mL ($R^2 > 0.99$) for pC and pCS, respectively, which are physiologically relevant. Intra- and inter-day precision and accuracy, autosampler stability (24hours at 4°C), and benchtop stability (8hours at room temperature) were within acceptable limits.

Conclusion: This is a novel assay capable of simultaneously quantifying both pC and pCS in HepaRG culture medium. This assay is being utilized in cellular toxicokinetic studies of pCS.

2D Descriptors as Modulators of Ligand Efficiency (LipE) metrics of Macrocytic Histone Deacetylase 1 (HDAC1) Inhibitors in the treatment of Acne vulgaris

Adeola Kola-Mustapha¹, Muhabat Raji¹, George Ambrose²

¹Alfaisal University Riyadh Saudi Arabia, ²University of Ilorin Teaching Hospital, Ilorin, Nigeria

Abstract

Purpose: The effectiveness of LipE is currently being used in the field of pharmaceutical sciences as a concept of drug design and formulation to simultaneously evaluate the effect of changes in physicochemical characteristics on both bioactivity and lipophilicity. Previous studies have shown that varying lipophilicity in a series of HDAC1 inhibitors will affect both protein-ligand affinity and their drug-like properties¹. Therefore, the needs of correlating their structural characteristics with their corresponding LipE, to identify the two-dimensional (2D) physicochemical properties involved in the lipophilicity of these compounds and thus help in designing better candidate drugs against HDAC1 in the treatment of acne vulgaris.

Methods: This is achieved by developing a model of quantitative structure-property relationship (QSPR) with HDAC inhibitors². Among the various 2D physicochemical descriptors that were considered as inputs to the model, three variables were selected using the genetic algorithm subset selection method (GA) while four variables were selected adopting the stepwise subset selection methods.

Results: The built-in models (Genetic Algorithm-Multiple Linear Regression (GA-MLR) and Stepwise-Multiple Linear Regression (S-MLR)) were robust and predictable with correlation factors (R^2) of 0.80217 and 0.98268 training sets of GA-MLR and S-MLR respectively. The accuracy of the proposed MLR models were demonstrated using the following evaluation techniques: cross-validation, validation through an external testing set and Y-randomization. Based on the outcome of the QSPR models results, the LipE of selected HDAC1 inhibitors had positive correlation with GATSp2 (Geary autocorrelation-lag2/weighted by atomic polarizabilities) descriptor which was derived from their structures.

Conclusion: The predictive ability of the models was found to be satisfactory and could be used for designing a similar group of anti-acne compounds.

References

1. Front Chem 2022 9: 815567.

2. Sci Technol Adv Mate 2022 2(1): 1-13.

A Novel Dissolution Model to Investigate the Release and Uptake of Oral Lymphotropic Drug Products

Malaz Yousef¹, Nadia Bou Chacra², Neal M. Davies¹, Raimar Löbenberg¹

¹Faculty of Pharmacy and Pharmaceutical Sciences, University of Alberta, Edmonton, AB, Canada, ²Faculty of Pharmaceutical Sciences, University of Sao Paulo, Sao Paulo, Brazil

Purpose:

Formulations of candidate lymphotropics are tailored by design towards intestinal lymphatic uptake as an alternative absorption route to the enteric-portal pathway.¹ However, standard dissolution tests estimate the aqueous release of drugs to ensure quality and performance but do not reflect whether they will be absorbed through the portal or the lymphatic circulation. This study aims at developing novel first-generation dissolution models to investigate the release and uptake of oral lymphotropic drugs and examine relevant formulation issues.

Methods: Dissolution of three commercial products of the lymphotropic drug; terbinafine (Terbinafina, APO-TERBINAFINE, and Lamisil) was tested using USP Apparatus II, IV, and our modified versions of both methods that contain a lymphatic compartment to mimic lymphatic uptake. The lymphatic space comprised a dialysis bag (molecular weight cut-off, MWCO:12-14kD, and 45mm-width) holding 5ml-Intralipid[®] (artificial chylomicrons that are enterocyte-formed lymphatic-carried lipoproteins which traverse drugs through the lymphatics). Standard conditions were applied and samples were taken at different time points up to 60 minutes, filtered through 0.2 μ nylon filters before being injected into the HPLC vials. Lymphatic vicinity samples were extracted before being analyzed.²

Results: We are able to examine simultaneously the rate and extent of release into simulated biological and lymphatic fluids using modified USP II or IV lymphocentric apparatus. The percentage dissolved over time revealed significant differences between the three products (Table

1). Each product was detectable in the lymphatic fluid with USP IV showing significant differences between products.

Conclusion: Our findings demonstrate that the developed lymphatic-focused dissolution models are able to examine formulations and factors potentially impacting chylomicron uptake. Establishing pharmaceutical lymphotropic performance testing that keeps pace with the increasing complexity of pharmaceutical products is critical for lymphotropic products. This model can be useful for formulation and manufacturing assessment and contribute to in-vitro bioequivalence guidelines of lymphotropic formulations.

References

1. J Pharm Pharm Sci 2021 24: 533-547
2. J Pharm Pharm Sci 2021 24: 50s

Table 1. Results of performance of the three terbinafine products (Terbinafina, Laboratorio.; APO-TERBINAFINE, Apotex, and Lamisil, Novartis) in simulated gastric fluid (pH =1.9) using modified USP II and IV dissolution apparatus for lymphotropic performance testing.

% absorbed of the 250-mg dose from the different products	Modified USP Apparatus II			Modified USP Apparatus IV		
	Terbinafina	APO-TERBINAFINE	Lamisil	Terbinafina	APO-TERBINAFINE	Lamisil
Absorption into blood circulation (% of drug in Vessel)	83.17	71.69	87.90	101.93	11.49	83.93
Lymphatic Uptake (% of drug in Intralipid [®])	2.58	1.71	2.32	2.14	0.21	1.16
Total amount absorbed	85.75	73.40	90.22	103.107	11.70	85.09

Microparticles-based formulations for a synthetic peptide EP80317 targeting CD36

Marie-Lynn AL-HAWAT¹, David N. Huynh¹, Mukandila Mulumba¹, Sylvie Marleau¹, Simon Matoori¹

¹Université de Montréal

Purpose. An innovative approach to the use of microparticles for peptide delivery to enhance bioavailability has emerged over the last decade. EP80317 (Haic-DMrp-DLys-Trp-DPhe-Lys-NH₂), a peptide ligand of the CD36 receptor, exerts cardioprotective activities, yet translational studies are hindered by the peptide rapid elimination from circulation. The objective of the present study aimed to assess in vitro release profile of different microparticle formulations in the absence and presence of serum.

Method. EP80317 (10^{-4} M in PBS) was incubated at 37°C with 10 mg silica, aluminosilicate, polyacrylic acid microparticles-1 (PaM1) or -2 (PaM2) for 0, 15, 45, 180, 360, 1440, 2880, 10080 minutes. Supernatants were assessed by fluorimetry (λ_{exc} 280 nm, λ_{em} 350 nm) and replaced by fresh PBS. In the presence of 10% FBS, supernatants were filtered on Amicon 50K. All assays were performed in triplicates.

Results. Diameters of the microparticles were determined using a laser diffraction analyzer (n=3), with median values ranging from 48,6 to 50,2 μ m for silica, 13,9 to 14,54 μ m for aluminosilicate, 690,4 to 694,4 μ m for PaM1 and 158,5 to 158,9 μ m for PaM2. The initial burst release of EP80317 from silica was $14 \pm 1\%$, followed by a sustained release of the peptide reaching, after a week, $72 \pm 3\%$. In contrast, aluminosilicate did not retain EP80317. PaM1 and PaM2 followed similar release profiles, with initial bursts of EP80317 of $48 \pm 2\%$ and $31 \pm 3\%$, respectively. In the presence of serum, the initial burst was greater than in PBS, $46 \pm 0,1\%$ and $69 \pm 3\%$ for silica and PaM2, respectively. EP80317 reached a plateau by 45 minutes.

Conclusion. Microparticles showed a progressive release of EP80317 after the initial burst in PBS except for aluminosilicate. In the presence of serum, the initial burst of the peptide was higher, and a plateau was quickly reached.

Data-driven development of lipid-based nanoparticles for oral drug delivery application

Zeqing Bao¹, Fion Yung¹, Pauric Bannigan¹, Christine Allen¹

¹Leslie Dan Faculty of Pharmacy, University of Toronto

Purpose:

Lipid-based nanoparticles (NPs) are an advanced drug delivery system composed of excipients that are “generally recognized as safe (GRAS)”. Lipid-based NPs have played a significant role as a platform for mRNA-based COVID-19 vaccine delivery. Despite their successful applications in macromolecule delivery, lipid-based NPs are relatively underexplored as a method to encapsulate small molecules. In particular, solid lipid NPs (SLNs) and nanostructured lipid carriers (NLCs) have potential in the delivery of lipophilic drugs, that are generally not amenable to liposome formulation. Here, we describe a miniaturized and automated screening pipeline to fast-track the design of SLNs and NLCs using GRAS excipients for hydrophobic molecule encapsulation.

Methods:

NP formulation was miniaturized (from 18 to 0.3 mL/batch) using a liquid-handling robot based on the nanoprecipitation method. The generated results were modelled by supervised machine learning regressors (e.g., XGBoost). The optimal models were then interpreted to map the relationship between the composition, properties and performance of NPs. Lead candidate formulations were then scaled up using a bench-scale nanoprecipitation method [1]. The pharmacokinetics and biodistribution of selected NP formulations were evaluated following oral administration to female Sprague Dawley rats (20 mg/kg, free access to food).

Results:

In total 96 SLN/NLC (n=3) encapsulating a model hydrophobic drug were prepared and characterized using the developed automated workflow. Lead candidate formulations identified were translated to bench-scale nanoprecipitation methods. The scaled-up NPs (100-200 nm, Figure 1) were found to significantly increase the apparent drug aqueous solubility. The NPs were further tested *in vivo* and resulted in a significantly improved pharmacokinetic profile compared to free drug.

Conclusion:

This approach enables accelerated evaluation of many formulation parameters with the use of minimal materials, in comparison to traditional formulation development. Lead candidate formulations identified using this data-driven approach improved the apparent solubility, chemical stability, and pharmacokinetics of a model hydrophobic compound.

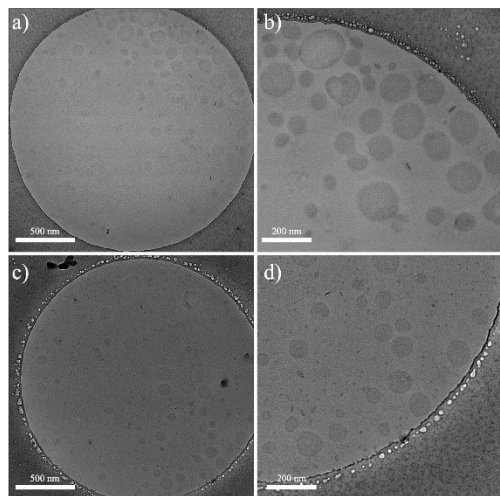


Figure 1. Representative cryo-EM images of the solid lipid nanoparticles (a and b)/nanostructured lipid carriers (c and d) showing a general spherical morphology. The scale bars represent 200 or 500 nm as indicated in the images.

References

[1] Molecules 2020 25: E4781

TARGETING GLIOBLASTOMA INVASION AND SURVIVAL WITH CANNABIS-DERIVED FLAVONOIDS

Akeem Gardner¹

¹Canurta Inc, Mississauga, ON

Introduction: Cannflavins A and B, hemp-derived flavonoids, exhibit anti-inflammatory, neuroprotective, and potential anti-cancer properties. Our group discovered their ability to inhibit TrkB receptor activation by BDNF, a pathway implicated in brain tumor biology. We investigated whether cannflavins affect glioblastoma (GBM) survival and migration.
Material &

Methods: We conducted alamarBlue and lactate-dehydrogenase (LDH) assays on U87-MG and A-172 GBM cell lines to assess cell viability and cytotoxicity at varying concentrations (10, 20, and 50 μM). Scratch assays evaluated cannflavins' impact on cancer migration (10 and 20 μM).

Results: Cannflavins A and B decreased cell viability in a dose and time-dependent manner. A-172 cells treated with 50 μM Cannflavin A for 24 hours showed a 61% reduction in viability ($p < 0.0001$; one-way ANOVA with respective vehicle control condition, $n=9$) and 5.16% LDH release (1.08 SEM; respective to lysis buffer positive control, $n=6$). Preliminary results indicate that 10 μM Cannflavin A reduced the A-172 cell migration to "wound area" after 24-48 hours compared to control.

Conclusion: Our study is an initial preclinical characterization of cannflavins against GBMs, aiming to position them as therapeutic candidates for brain tumors and other TrkB-driven cancers.

Category

Biomedical sciences

References

1. Barrett, M.L., Gordon, D., Evans, F. (1985) Isolation from Cannabis sativa L. of cannflavin - a novel inhibitor of prostaglandin production. *Biochem. Pharmacol.* 34, 2019-2024.
2. Erridge, S., Mangal, N., Salazar, O., Pacchetti, B., Sodergren, M.H. (2020) Cannflavins - From plant to patient: A scoping review. *Fitoterapia*, 146, 104712.
3. Holborn, J., Walczyk-Mooradaly, A., Perrin, C., Alural, B., Aitchison, C., Borenstein, A., Khokhar, J.Y., Akhtar, T.A., Lalonde, J. Inteference of neuronal TrkB signaling by cannabis-derived flavonoids cannflavins A and B. bioRxiv preprint: <https://www.biorxiv.org/content/10.1101/2022.02.03.478734v2>.
4. Pinheiro, K.V., Alves, C., Buendia, M., Gil, M.S., Thomaz, A., Schwartzmann, G., de Farias, C.B., Roesler, R., Bowman, R.L., Wang, Q., Carro, A., Verhaak, R.G., Squatrito, M. (2017) Targeting tyrosine receptor kinase B in gliomas. *Neuro. Oncol.*, 19, 138-139.

Identifying the target(s) of a potent small molecule immunomodulator using Jurkat cells

Yasser Tabana¹, Shima Shahbaz¹, Jenny C.H. Lin¹, Dinesh Babu¹, Marawan Ahmed¹, Ramanaguru Piragasam⁴, Richard Fahlman¹, Tae Chul moon¹, Shokrollah Elahi¹, Frederick G. West¹, Arno Siraki¹, Khaled Barakat¹

¹Universiy of ALberta

Background: Immunotherapeutic approaches utilize components of a patient's own immune system to target cancer cells selectively. Our laboratory has identified a small molecule (Compound B) that has significant activity in modulating the immune system.

Purpose: A comprehensive investigation is ongoing to identify and validate the target(s) and pathway(s) associated with the observed activity of Compound B. **Methods:** The immunostimulatory ability of Compound B was investigated using Jurkat cells. The levels of cytokines and chemokines produced in response to Compound B treatment were measured using enzyme-linked immunoassay (ELISA) and V-plex Plus kits from Meso Scale Discovery (MSD). The possible targets of Compound B were identified using pull-down and LCMS analysis.

Results: The results showed that Compound B significantly increased the production of several cytokines, including IL-13, IL-6, IL-2, IL-1b, IL-4, and IL-8. The LCMS results revealed 658 detected proteins, with 21 significant proteins identified based on P values < 0.05. CDK6 was selected as a potential target for further analysis, as it is on the significant list and previous reports suggest that inhibiting CDK6 is involved in immunomodulatory effects.

Conclusion: Our study showed the immunostimulatory activities of Compound B and possible immunological targets. A future direction will be to validate the molecular targets responsible for its immunological activities. This project will result in a complete understanding of the

mechanism of action of Compound B, which can potentially lead to the discovery of novel cancer immunotherapeutic small molecule.

Improving the oral bioavailability of a BCS class IV compound by nanoemulsion and nanosuspension: A challenge

**Badiss Meddeb¹, Mihaela Friciu¹, Isabelle St-Jean¹, Jean Laverdière¹,
Detty Balufu Kayaya¹, Grégoire Leclair¹, Valérie Gaëlle Roullin¹**

¹Faculty of pharmacy, Université de Montréal, Montreal, QC

Purpose: Nanoemulsion and nanomilling were compared as means to improve the oral bioavailability (<1%) of a previously proved safe (phase 1 clinical trial) BCS class IV drug.

Methods: A large library of excipients (solvents, vegetable oils and surfactants) was screened for drug solubility using a HPLC-UV validated method. Best solubilizing excipients were used to formulate Water-in-Oil type emulsions. Nanoemulsions were obtained by high speed homogenization (Polytron®), completed with high pressure homogenization (Emulsiflex™ C3). Nanosuspensions were prepared by mixing different polymeric excipients and surfactants with drug powder in water; zirconia beads were then added and the whole system was placed in rotation for 72h (50 rpm, Roller Mill™). Nanoformulations were characterized for size, polydispersity (DLS, Laser Diffraction) and stability. Drug content was assessed by HPLC-UV.

Finally, 2 nanoemulsions and 4 nanosuspensions were tested in rats (n=3/group) against an IV formulation. Samples were taken over of 24h period and analyzed by HPLC-MS/MS with data analyzed using Kinetica®.

Results: Among 32 evaluated W/O nanoemulsions, those formulated with an organic phase consisting of sunflower oil+soy lecithin or sesame oil+span 80 and the same water-soluble solvent as the internal phase displayed the best stability (up to 7 hours). Process parameters, such as phase ratio, homogenization pressure and time, were optimized for 3

nanoformulations, with encapsulation rates up to $105 \pm 1\%$.

Of 19 prepared nanosuspensions, nine stable ones with $D_{90} < 230$ nm were retained. Best formulations included HPC-SSL, PVP K29/30 and HPMC-E5 polymers, leading to production yields of $80 \pm 5\%$.

Absolute bioavailability of one nanoemulsion was 2.5% (non-biologically significant). Plasma concentrations of the other nanoemulsion and nanosuspensions were too low to be accurately detected.

Conclusion: Despite promising physicochemical features, neither nanoemulsion nor nanomilling techniques improved the oral bioavailability of this BCS class IV drug. Other nanoformulations involving lipidic excipients are currently explored.

Dolutegravir (DTG)/Bictegravir (BTG)-Based Antiretroviral Therapy Dysregulates Drug and Folate Transport Pathways in the Brain

Shirley (Chang) Huang¹, Md. Tozammel Hoque¹, Reina Bendayan¹

¹university of toronto

Purpose: HIV+ individuals are susceptible to neuropsychiatric symptoms associated with antiretroviral drugs (ARVs). Drug efflux transporters, P-glycoprotein (*Abcb1a/P-gp*) and breast cancer resistant protein (*Abcg2/Bcrp*) expressed at the blood-brain barrier (BBB) play a critical role by limiting access to many xenobiotics including drugs and toxins into the brain and maintaining the homeostasis of the central nervous system. Similarly, folate transporters including Reduced Folate Carrier (*Slc19a1/Rfc*), Proton-Coupled Folate Transporter (*Slc46a1/Pcft*) and Folate Receptor Alpha (*Folr1/Fra*) at the choroid plexus (CP) and BBB, are important in mediating cerebral folate transport. Previous findings from our group suggested a potential interaction between DTG and folate transporters at the placenta. We hypothesized that first-line ARVs dolutegravir (DTG) and bictegravir (BTG) dysregulate these transporters at the BBB and CP.

Method: C57BL/6 mice were administered orally either with DTG (5mg/kg/day); BTG (5mg/kg/day); DTG + backbone (tenofovir alafenamide (50mg/kg/day) + emtricitabine (33.3mg/kg/day) or BTG + backbone for 14 days. *Abcb1a*, *Abcg2*, *Slc19a1*, *Slc46a1*, *Folr1* gene expression was quantified by qPCR in isolated mouse brain capillaries (BBB) and CP.

Results: Chronic treatment of mice with DTG or BTG significantly downregulated *Abcb1a* and *Abcg2* gene expression in isolated brain capillaries. Additionally, DTG treatment downregulated *Folr1* while BTG treatment downregulated *Slc19a1*, *Slc46a1* and *Folr1* in mouse brain capillaries. Administration of DTG+backbone or BTG+backbone in mice significantly downregulated *Slc19a1* and *Slc46a1* at the CP, and BTG + backbone also downregulated *Folr1* in mouse brain capillaries.

Conclusions: Our findings suggest that DTG and BTG based combined antiretroviral therapy (cART) dysregulates drug efflux transporters and folate transporters/receptor at BBB and CP, which may contribute to cART-associated neuropsychiatric adverse effects by inducing cerebral folate deficiency. These interactions may also contribute to long-term HIV-associated neurocognitive disorders by increasing brain exposure of ARVs that are substrates to P-gp and/or Bcrp. (*Supported by CIHR and OHTM*)

Re-development of Glybera: A Novel Gene Therapy for Lipoprotein Lipase Deficiency

Neel Mehta¹, Rénaud Gilbert^{2, 3}, Parminder S. Chahal², Maria J. Moreno⁴, Nasha Nassoury², Nathalie Coulombe², Viktoria Lytvyn², Mario Mercier⁴, Dorothy Fatehi⁴, Wendy Lin¹, Emily M. Harvey¹, Lin-Hua Zhang⁵, Nazila Nazemi-Moghaddam², Seyyed Mehdy Elahi², Colin J.D. Ross^{1, 5}, Danica B. Stanimirovic⁴, Michael R. Hayden¹

¹Centre for Molecular Medicine and Therapeutics, BC Children's Hospital Research Institute, Department of Medical Genetics, University of British Columbia, Vancouver, BC, ²Department of Production Platforms & Analytics, Human Health Therapeutics Research Centre, National Research Council Canada, Montréal, QC, ³Department of Bioengineering,

McGill University, Montréal, QC, ⁴Department of Translational Biosciences, Human Health Therapeutics Research Centre, National Research Council Canada, Ottawa, ON, ⁵Faculty of Pharmaceutical Sciences, University of British Columbia, Vancouver, BC

Purpose

Lipoprotein lipase deficiency (LPLD) is a monogenetic recessive disease resulting from mutations within the lipoprotein lipase (LPL) gene that lead to a complete lack of catalytically active LPL protein. LPLD is associated with severe hypertriglyceridemia and complications such as eruptive xanthomas and life-threatening pancreatitis. We previously contributed towards the development of Glybera, the first adeno-associated virus (AAV) gene therapy product to receive regulatory approval in the western world for the treatment of LPLD. However, Glybera is no longer marketed due to economical considerations. The aim of this study was to redevelop a more efficacious, cost-effective AAV gene therapy formulation for LPLD.

Methods

Novel AAV formulations were tested against Glybera in a mouse model of LPLD. All formulations were delivered intramuscularly at $1.0E+11$ gc/kg (LD) or $1.0E+12$ gc/kg (HD) ($n=3-4$ mice/group). Mice were followed for 80 days following treatment. Plasma triglycerides (Tg) were assessed throughout the study to determine efficacy. Transgene biodistribution, plasma biochemistry and tissue pathology were assessed at endpoint.

Results

We identified a novel formulation, pVR59, that resulted in significantly increased efficacy, associated with complete normalization of plasma Tg by study endpoint (105 ± 21 mg/dl, associated with a -99% decrease from baseline) compared to Glybera (3696 ± 523 mg/dl, associated with a -60% decrease from baseline) at the HD ($p\leq 0.05$). pVR59 treatment resulted in an approximate 3-, 5- and 12-fold increase in therapeutic hLPL transgene expression within plasma, skeletal muscle and liver respectively, compared to Glybera at the HD ($p\leq 0.05$). No local or systemic toxicity was observed following pVR59 treatment.

Conclusion

Our results highlight the feasibility of developing a superior AAV gene therapy product for the treatment of LPLD. The identification of a novel AAV formulation that is superior to Glybera at lower doses, when paired with recent advances in AAV manufacturing processes, will translate to increased safety, efficacy and lower manufacturing costs.